A THESIS
FOR THE DEGREE OF DOCTOR OF PHILOSOPHY

CHARACTERIZATION OF ANTIOXIDANT GENES FROM ABALONE (*Haliotis discus discus*) cDNA

Prashani Mudika Jayasooriya

Department of Marine Biotechnology
GRADUATE SCHOOL
CHEJU NATIONAL UNIVERSITY

2005. 12

CHARACTERIZATION OF ANTIOXIDANT GENES FROM ABALONE (*Haliotis discus discus*) cDNA

Prashani Mudika Jayasooriya
(Supervised by Professor Sang-Chul Chung)

A thesis submitted in partial fulfillment of the requirement of the degree of Doctor of Philosophy

2005. 12

This thesis has been examined and approved by

……

Chairperson of the supervising committee

You-Jin Jeon, Professor of Marine Biotechnology

……

Choon-Bok Song, Professor of Marine Biotechnology

……

In-Kyu Yeo, Professor of Marine Biotechnology

……

Moon-Soo Heo, Professor of Marine Biotechnology

……

Sang-Chul Chung, Professor of Marine Biotechnology

……

Date

Department of Marine Biotechnology
GRADUATE SCHOOL
CHEJU NATIONAL UNIVERSITY

CONTENTS

요약문

항산화 효소들은 체내에서 생명 유지를 위해 산화 환원 반응을 조절하는 중요한 역할을 한다. 이 논문에서는 까막전복으로부터 만들어진 cDNA library 로부터 중요한 항산화 효소로 알려진 catalase (aCAT), Cu,Zn-superoxide dismutase (aCu,Zn-SOD) 와 Mn-superoxide dismutase (aMn-SOD)에 대한 코딩 유전자의 서열을 분석하였다. 첫번째로, 전체 길이를 확인한 후 그 서열들은 기존에 data base 를 통해 비교되어졌고 구조와 기능이 유사한 다른 생물의 효소들과의 비교를 통해 보존된 서열이 확인되어졌다.

두 번째로, PCR 을 통해 코딩 서열을 증폭시키고 그 산물을 pMAL-c2X vector 내로 삽입시킨 후 *E. coli* BL21(DE3)나 K12(TB1)에 형질전환 시켜졌다. 그 각각의 재조합 단백질들은 IPTG 를 이용해 발현이 유도되어졌다. 그리고 발현된 단백질들은 최적 온도와 pH 그리고 열 안정성이 각각 진단되어졌다. 각각의 효소들에 대한 계통 수는 neighbour-joining 의 방법에 의해 시행되어졌다.

H_2O_2 에서 H_2O 와 O_2 로의 반응을 촉매하는 catalase 는 세포질내의 H_2O_2 의 독성을 제거하는 중요한 효소로 알려져 있다. 그 catalase 는 501 개의 아미노산을 코딩하는 1503 bp 의 ORF 로 구성되며 전복에서 true catalase 그룹인 것으로 확인 되어졌다. 그 catalase 의 specific activity 는 30,000 U/mg 이었다. pH 는 5.0 에서 10.5 까지 안정했고 열안정성은 70 °C 이하에서 안정하게 나타났다. 알려져있는 다른 22 개의 catalase 아미노산 서열과 비교했을 때 173 개의 잔기가 보존된 서열로 나타났고 34.5% 의 homology 를 보였다. 그리고 aCAT 는 Pacific white shrimp 의 CAT 와 가장 높은 유사성을 나타냈다.

Superoxide dismutase (SOD)는 superoxide (O_2^-)과 반응하는 하나뿐인 항산화 효소이다. SOD 는 위치와 활성 금속이온에 따라 구분되어진다. aCu,Zn-SOD 는 154 개의 아미노산을 코딩하는 465 개의 염기로 구성되고 pI 값이 5.5, 분자량이 16 kDa 이다. aCu,Zn-SOD 의 최적 온도는 37 °C 이며 그것은 70 °C 에서 활성을 잃어버렸다. 그리고 산성 pH 인 3.5 – 6.5 범위에서 활성을 가졌다. 47 개의 다른 종의 SOD 와 비교했을 때 48 개의 아미노산이 보존되었고 29%의 homology 를 보였다.

Cu 와 Zn 이온의 부착을 위한 모든 잔기들이 aCu,Zn-SOD 에 보존되어있었다. 계통수로 볼 때 aCu,Zn-SOD 는 *H. diversicolor* 의 것과 가까웠고 이것은 다른 전복의 일종으로 두 종간의 관계가 진화적으로 가까웠음을 보여준다.

Mn-SOD 는 세포질내로 생산되어지지만 미토콘드리아의 post-translationally 에 중요하다. aMn-SOD 는 226 개의 아미노산을 코딩하는 690 개의 염기로 구성되며 25 개의 아미노산으로 구성된 신호서열을 포함한다. 발현된 aMn-SOD 의 분자량은 25 kDa 이고 최적온도는 37 °C 이다. aMn-SOD 도 aCu,Zn-SOD 와 마찬가지로 산성 pH 에서 활성을 가졌다. 그 효소는 80 °C 에서 활성을 잃었다. aMn-SOD 의 아미노산 서열은 35 개의 다른 서열과 비교했을 때 fresh water snail (*Biomphalaria labrata*)의 Mn-SOD 와 가장 가까웠다.

이 연구에서는 까막전복으로부터 CAT, Cu,Zn-SOD 와 Mn-SOD 의 유전자를 분석하고 클로닝하여 과잉발현을 유도하였으며 그 발현된 단백질을 정제하여 각각의 특성을 분석하였다. 각각의 염기서열분석은 무척추동물의 항산화 효소와 그들의 진화 상에서 비교에 의한 게놈 연구에 기여할 수 있다.

List of Figures

INTRODUCTION

Although oxygen is essential to life as a part of normal metabolism, its access can give rise to a variety of reactive oxygen species (ROS). Under normal conditions, the body is well equipped with a variety of mechanisms that serve to inactivate the extra ROS. However, under certain conditions, where these mechanisms are faulty or the body has been exposed to environmental chemicals, irradiation, iron loading, and other similar factors, the elevated ROS levels can cause a variety of diseases and could even lead to death. They not only damage biological molecules like protein and DNA but also lead to cell death and thereby become a cause to a tremendous number of diseases including cancer, alzheimer and arthritis. ROS are formed in the body as toxic by-products of oxidative metabolism (Ken et al., 2003). These include superoxides, hydrogen peroxide (H_2O_2), hydroxyl radicals and singlet oxygen. Cells have developed multilayered interdependent antioxidant system as a defense against oxidative injury. This system comprises enzymatic and non-enzymatic components. Superoxide dismutase, catalase and glutathione peroxidase are the enzymes that catalyze the dismutation of the ROS. Antioxidant enzymes play a major role in protecting organisms from the potentially deleterious effects of ROS. They contribute towards strengthening the defense mechanism in cells, and are studied in detail in several aquatic organisms (Nakano et al., 1995).

Catalase is an antioxidant enzyme in the cellular protection system and catalyzes the decomposition of hydrogen peroxide to oxygen and water

(Thuy et al., 2004). It is also found in all aerobic cells. The level of catalase expression is highly tissue specific. The highest levels are found in liver, kidney and blood while the lowest levels are found in connective tissues and brain (Chen et al., 2004). Presence of catalase is important in the prevention of toxic wastes, which are harmful to cells. Human acatalasemia is a genetic example of catalase deficiency, which has been observed in Japanese individuals (Ogata, 1991).

Most catalases exist as tetramers of approximately 65 kDa subunits (Bravo et al., 1999) and classified under three sub classes namely typical, catalase peroxidases and manganese catalases. Each of the four subunits contains Fe^{3+} prosthetic heme groups (protoporphyrin IX), which is exposed through a 26 A^o long and 17 A^o wide funnel shaped channel. The heme group is proved to be responsible for the enzymatic activity of catalase. Catalytic mechanism of catalase is a two-step reaction (Deisseroth and Dounce, 1970). In the first step, the heme Fe^{3+} reduces a hydrogen peroxide molecule to water and generates a covalent $Fe^{4+}=O$ oxyferryl species with a porphyrin π-cation radical, which is referred as compound I and in the second step, compound I oxidizes a second peroxide molecule to molecular oxygen and releases the ferryl oxygen species as water (Chance, 1949). Catalase enzyme complex also binds the reductant NADPH (Fita and Rossmann, 1985) yet, hydrogen peroxide is the source of both oxidative and reductive potential during the normal catalytic cycle.

Catalase cDNAs have been isolated from number of eukaryotic organisms including human, rat, cattle, yeast, mice, and sweet potato (Hass et al., 1991). Most of these catalases share a high degree of amino acid sequence identity. In comparison with catalases from mammalian and bacterial sources, there is little information available on mollusk catalase, especially on its biochemical properties. Gerhard et al. confirmed that other than amphibia (Dadras et al., 1996), little has been reported about the structure or regulation of catalase in non-mammalian vertebrates (Gerhard et al., 2000).

Superoxide dismutases (SOD) are metalloenzymes in aerobic organisms, which play another crucial role in protecting organisms against the toxic wastes caused by ROS, in particular superoxide radicals ($O_2^{\cdot -}$) (Liu et al., 2002). It catalyses the dismutation of superoxide radicals to molecular oxygen and hydrogen peroxide (Wang et al., 2005). Although $O_2^{\cdot -}$ is a mild reactant, it can cause direct or indirect damage to the membranes and DNA, when it is protonated to hydroxyl radical ($HO^{\cdot}$) or dismutated to H_2O_2 (Birnboim and Kanabus-Kamnika, 1985). The reported medical applications of SOD include anti-inflammation, prevention of oncogenesis & tumor growth, and protection against reperfusion damage of ischemic tissue (Garcia –Gonzalez and Ochoa, 1999; Kondo et al., 1999). It has also been proposed that bacterial Cu,Zn-SOD is involved in pathogenic infections and survival at the stationary phase of growth while being resistant to oxidative stress (Kho et al., 2004). Moreover, Fridovich (1986) reported that organisms lacking

SODs exhibit a decreased growth rate, short life span, hypersensitivity towards redox cycling compounds (such as paraquat and quinines) and accelerated spontaneous mutagenesis resulting high death rates.

SODs are classified into several forms and can be distinguished by their primary structure, cellular compartmentalization, primary function and the metal required for activity (Wright et al., 2002). Three distinct groups depending on the metals identified in their active sites are Cu,Zn-SOD, Mn-SOD, and Fe-SOD. Cu,Zn-SODs are widely distributed in eukaryotes, whereas Mn-SOD and Fe-SOD enzymes are predominantly found in mitochondria or prokaryotes (Fridovich, 1986). Recently a variety of other forms of SODs have been identified in bacteria. These include a nickel-containing isozyme (Kim et al, 1998a) and hybrid isoforms containing iron and zinc (Kim et al., 1998b). Among Cu,Zn-SOD, cytosolic Cu,Zn-SOD and glycosylated extracellular Cu,Zn-SOD has been found in eukaryotes (Jeong et al., 2001) and is also reported to have a widespread distribution in a variety of cells.

The genomic sequence for Cu,Zn-SOD has been identified in the rat (Kim et al., 1993), mouse (Benedetto et al., 1991) and human (Levanon et al., 1985). Fukuhara et al. (2002) have carried out a comprehensive study on structure, molecular evolution, and gene expression of Mn- and Cu,Zn-SOD on eight primate species. Cu,Zn-SOD coding sequences have been cloned from many diverse organisms and expressed in various systems such as *E.coli* (Bricker et al., 1990), *Lactococcus lactis* (Xiang et al., 2000), yeast

(Hallewell et al., 1991), *Drosophila melanogaster* (Reveillaud et al., 1991) and even in transgenic mice (Ceballos et al., 1991). Further, molecular cloning of Cu,Zn-SOD from three different mollusk species have been reported by Geret et al. (2004). Although coding sequence for Cu,Zn-SOD of *Haliotis diversicolor supertexta* (AAY18806) is available, limited studies on cloning of Cu,Zn- SOD from Mollusks led this study to clone, sequence and express aCu,Zn-SOD in *E. coli,* and compare them with other known Cu,Zn-SOD sequences to identify conserved regions that may be useful in elucidating its structure-functional relationship.

Out of the SODs found in eyukaryotes (cytosolic Cu,Zn-SOD, glycosylated extracellular Cu,Zn-SOD and mitochondrial Mn-SOD), Mn-SOD is particularly important as it is located in mitochondria and represents the first line of defense against superoxide radicals produced as byproducts of oxidative phosphorylation (Beyer et al., 1991). In eukaryotic cells, Mn-SOD is synthesized in the cytosol and imported post-translationally into the mitochondrial matrix (Bannister et al., 1987). Mitochondria is an important site for the single-electron reduction of O_2 to $O_2^{-\cdot}$ Therefore, Mn-SOD is thought to be a major scavenger of damaging ROS metabolites in the mitochondrial matrix (Ken et al., 2005).

Mn-SOD is a homotetramer of about 23 kDa subunits and localized in mitochondrial matrix of aerobic cells. Interestingly, its amino acid sequence is distinctly different from the amino acid sequence of Cu,Zn-SOD (Bannister et al., 1987). Mn-SOD has been shown to play a major role in

promoting cellular differentiating and tumorgenesis (St.Clair et al., 1991) and in protecting cells against hyperoxia-induced pulmonary toxicity (Wispe et al., 1992). Further, overexpression of the protein has well-documented anti-apoptotic effects (Pani et al., 2000; Bernard et al., 2001; Drane et al., 2001) and its deletion has lead to neurodegeneration and cardiomyopathy in mice (Lebovitz et al., 1996; Melov et al., 1998). Many scientists have summarized the role of Mn-SOD in protection against ROS and their physiological function in several excellent reviews (Fridovich, 1995; Bannister et al., 1987; McCord and Fridovich, 1988; Oberley and Buettner, 1979). The complete genomic structure of Mn-SOD for human (Church et al., 1992; Wan et al., 1994), rat (Ho et al., 1991), and mouse (DiSilvestre et al., 1995) has been determined. Also, partial identification and characterization of bovine Mn-SOD has described by Meyrick and Magnuson (1994). However, available information on Mn-SOD from invertebrates is not sufficient.

In this study, cDNA coding for three antioxidant genes; catalase, Cu,Zn-SOD and Mn-SOD from disk-abalone (*Haliotis discus discus*) were sequenced, cloned, expressed and characterized. The isolated sequences were compared with that of other species available in the public database and attempts were made to build structure-functional relationship of the amino acid sequences.

Part I

Cloning, expression, purification and characterization of catalase from abalone (*Haliotis discus discus*) cDNA

1. ABSTRACT

Catalase is an antioxidant enzyme, which plays a crucial role within the cellular protection system. It facilitates the degradation of hydrogen peroxide, which is a reactive oxygen species, into oxygen and water. Biochemical information on mollusk catalase is however, insufficient. A gene coding for putative catalase of the disk abalone (*Haliotis discus discus*) was selected from the cDNA library (derived from digestive gland) and the full-length was sequenced using 3 internal primers. The full-length cDNA contained 2,733 bp whilst the coding sequence was 1,503 bp. The catalase coding sequence was amplified with two designed primers and cloned into pMAL-c2X. The recombinant abalone catalase was expressed in *E. coli* in the soluble form (belonging to typical catalases) and the molecular weight was reported to be 56 kDa. The specific activity of expressed catalase was 30,000 U/mg towards hydrogen peroxide and was stable in a broad range of pH (5.0-10.5). The enzyme has its optimum activity at 37 ^{o}C and was inactivated when heated at 70 ^{o}C for 20 min. Phylogenetic studies revealed that aCAT is closer to catalase of pacific white shrimp among the available catalase amino acid sequences in the public database.

2. MATERIALS AND METHODS

Cloning and sequencing of the gene encoding aCAT:

A clone with expected function of catalase (aCAT) was selected from abalone cDNA library. The plasmid DNA of the putative aCAT was isolated by the Accuprep^{TM} plasmid extraction kit (Bioneer Co., Korea). The full-length sequence was determined by three sequencing reactions from 5' end using three primers (GTTCTACACTGAAGACGGC, CGGCGCATATGGTGACAGG and CGCTCCAAGAATGAGTATGTG). After deriving the full length, the sequence was compared against the National Center for Biotechnology Information (NCBI) databases by BLAST-X

Cloning the coding sequence of aCAT into pMAL expression vector:

Having checked the restriction enzyme sites of the aCAT sequence, a pair of primers was designed for cloning the coding sequence of the aCAT into expression vector, pMAL-c2X (New England Biolabs, USA). The sense amplification primer was designed as 5'-GAGAGAGATCTAGAATGGCGACCAGGGATAAGGC-3' having a *Xba* I site and an antisense primer 5'-GAGAGAGAAAGCTTCTATGGCTCCACTTTCAAGGCGT-3' containing a *Hind* III site. In a total of 50 µl of PCR reaction, 5 units of Ex Taq polymerase (Takara Korea Biomedical Inc., Korea), 5 µl of 10X Ex Taq buffer, 4 µl of 2.5 mM dNTP, 50 ng of template, 50 pmol of each primer were used. After initial incubation at 94 ^{o}C for 2 min, 25 cycles were carried

out with 30 sec denaturation at 94 ^{o}C, 30 sec of annealing at 55 ^{o}C, and 90 sec of elongation at 72 ^{o}C, followed by a final extension at 72 ^{o}C for 5 min. The PCR product was analysed using 1% agarose gel and ethidium bromide staining. Thereafter, it was purified by the Accuprep^{TM} gel purification kit (Bioneer Co., Korea) and digested with *Hind* III and *Xb*a I restriction enzymes. The expression vector, pMAL-c2X, was digested with the same restriction enzymes as the PCR product and dephosphorylated with calf intestine phosphatase (NEB, USA) according to the vendor's protocol. Thereafter, the vector and PCR product was purified by a 1% agarose gel using Qiaex-II gel purification Kit (QIAGEN Inc., USA).

Ligation was carried out at 16 ^{o}C, overnight with 100 ng of pMAL-c2X vector, 70 ng of PCR product, 1 µl of 10X ligation buffer and 0.5 µl 1X T4DNA ligase (Takara Korea Biochemical Inc., Korea). The ligated product was transformed into XL1 cells. The correct recombinant confirmed by colony cracking, restriction enzyme digestion and sequencing was transformed into the competent cells; *E. coli* BL21 (DE3).

Overxpression of catalase:

The recombinant enzyme was overexpressed in *E. coli* BL21 (DE3) cells in the presence of isopropyl-ß-thiogalactopyranoside (IPTG). A volume containing 10 ml of starter culture was inoculated into 100 ml Luria broth with 100 µl ampicillin (100 mg/ml) and 10 mM glucose (2% final concentration) and kept at 37 ^{o}C with 200 rpm until OD_{600} approached 0.5. The culture was then shifted to 20 ^{o}C for 15 min prior to induction with 1

mM IPTG at the final concentration. After 3 hrs of induction, the cells were cooled on ice for 30 min and harvested by centrifugation at 4000 rpm for 20 min at 4 ^{o}C. The cells were re-suspended with 5 ml column buffer (Tri-HCl, pH 7.4, 200 mM NaCl, 0.5 M EDTA) and frozen in liquid nitrogen and stored in -70 ^{o}C freezer.

Purification of catalase:

After thawing, the bacterial cells were placed in an ice-water bath and sonicated in short pulses of 10 sec for 6 times. Having centrifuged at 9000 x g for 30 min at 4 ^{o}C, the supernatant was diluted with 1:5 column buffer. The pMAL^{TM} protein fusion and purification system was followed. In brief, amylose resin was poured into a 1 x 5 cm column and washed with 8 x column volumes of column buffer. The diluted crude extract was loaded at a flow rate of 1 ml/hr. The column was then washed with 12 x column volumes of column buffer and the fusion protein was eluted with elution buffer (column buffer + 10 mM maltose). The elute was collected in 500 µl fractions. The eluted protein content was measured by UV absorbance at 280 nm.

Gel electrophoresis :

SDS-PAGE was performed according to the standard procedure for discontinuous SDS-PAGE. The stacking and separating gels were prepared at 5 and 12% respectively and the gel was stained with Coomassie blue.

Catalase activity assay and determination of protein concentration:

Catalase activity was assayed spectrophotometrically at 25 ^{o}C by the method of Muller (1985). The purified enzyme (20 µl) dissolved in 100 µl phosphate-buffer saline (0.1 M, pH 5.0) was mixed with 20 µl of H_2O_2 (10 mM) in a 96 Microwell Plate, and incubated at 37 ^{o}C for 5 min. After the incubation period, 30 µl 2,2-Azino-bis (3-ethylbenzthiazolin)-6-sulfonic acid (1.25 mM) and 30 µl peroxidase (1 unit/ml) were added to the mixture and was incubated again at 37 ^{o}C for 10 min. The incubation of ABTS with peroxidase resulted in the production of the radical cation of ABTS, which is blue-green and can be read using the enzyme linked immunosorbent assay (ELISA) reader at 405 nm. The enzyme assay was carried out in triplicate and the mean velocities were reported. One unit of activity was defined as 1 µmol H_2O_2 decomposed/min under the assay conditions. Protein concentration was determined by the procedure of Lowrey et al. (1951) using bovine serum albumin as the standard.

In order to conduct optimal temperature, each reaction was carried out 30, 37, 40, 50, 60, 70, 80, 90 and 100 ^{o}C and relative activity was determined. The optimal pH of the aCAT, was determined with acetate buffer (pH 3.5 - 5.5), phosphate buffer (pH 6.5 and pH 7.5) and glycine-NaOH buffer (pH 8.5 - 10.5).

Analysis of nucleotide and amino acid sequences:

Nucleotide sequence analysis was performed with the DNAssit program (version 2.2). The NCBI BLAST program (http://www.ncbi.nlm.nih.gov) was used to search for nucleotide and protein sequences similar to the aCAT. Protein sequence analysis was performed with the CLUSTAL W Multiple Sequence Alignment Program (version 1.8, 1999). Phylogenetic relationship was determined by MEGA 3.0 (Kumar, et al., 2004) program. The phylogenetic tree was constructed using the Neighbour-joining method.

3. RESULTS

```
                    CACTCTCCTACCCATGCAAGTAGCTTGGTCTGCGTAACATCGACAAGCCCTCAACGAACT          60
GATCCTGGTTTATGCAACCGGTAATTTGACCTGAATAAGCTATACGTCAGAGGAAAGTTCTGCGCGTTTCTTCACTTCTTAATC  144
ATGGCGACCAGGGATAAGGCGTCCGAGCAGCTAAATGAATTCAGCAAAGGACAGAAGAAACCGGATGTCCTCACAACAGGCACA  228
M--A--T--R--D--K--A--S--E--Q--L--N--E--F--S--K--G--Q--K--K--P--D--V--L--T--T--G--T-
I----------------------------------N Terminal domain----------------------------------
GGTGCACCTGTGGGCCGTAAGACAGCCACAATGACTGTGGGACCACAGGGGCCTGTGTTGTTGCAGGACTTCGTGTTCACGGAC  321
G--A--P--V--G--R--K--T--A--T--M--T--V--G--P--Q--G--P--V--L--L--Q--D--F--V--F--T--D-
------------------------------------------------------------------------------------
GAGATGGCGCATTTCAACAGAGAGAGGATCCCTGAGAGAGTCGTGCATGCTAAAGGAGCAGGGGCGTTCGGCTACTTGGAAATA  396
E--M--A--H--F--N--R--E--R--I--P--E--R--V--V--H--A--K--G--A--G--A--F--G--Y--L--E--I-
-------------------------------------------I------------------------------------
ACACACGACATCACCAAGTATTGTAAAGCAAAGGTATTTGAACGTGTTGGCAAGAAGACGCCACTTGCTATCAGGTTTTCAACT  480
T--H--D--I--T--K--Y--C--K--A--K--V--F--E--R--V--G--K--K--T--P--L--A--I--R--F--S--T-
------------------------------------β barrel domain---------------------------------
GTAGGTGGTGAGAAGGGGTCGGCGGACACCGCCAGGGACCCCCCGGGGGTTCGCCATAAGTTCTACACTGAAGACGGCAACTGG  564
V--G--G--E--K--G--S--A--D--T--A--R--D--P--P--G--V--R--H--K--F--Y--T--E--D--G--N--W-
------------------------------------------------------------------------------------
GACCTGGTGGGCAATAACACTCCCaTCTTCTTCATAAGGGACCCTATGCTGTTCCCCAGCTTCATCCACACCCAGAAGAGAAAC  648
D--L--V--G--N--N--T--P--I--F--F--I--R--D--P--M--L--F--P--S--F--I--H--T--Q--K--R--N-
------------------------------------------------------------------------------------
CCCGTTACCAACCTGAAGGACCCCGATATGTTCTGGGACTTCATCACGCTGCGTCCTGAGACCACCCACCAGGTGGCCTTCCTC  732
P--V--T--N--L--K--D--P--D--M--F--W--D--F--I--T--L--R--P--E--T--T--H--Q--V--A--F--L-
------------------------------------------------------------------------------------
TTCTCGAACCGCGGGACCCCAGATGGTTATCGTCACATGAACGGCTATGGCAGCCACACTTTCAAGATGGTCAACGCCAAGGGG  816
F--S--N--R--G--T--P--D--G--Y--R--H--M--N--G--Y--G--S--H--T--F--K--M--V--N--A--K--G-
------------------------------------------------------------------------------------
GAGTGTGTGTACTGCAAGTTTCACTTCAAGACAAACCAAGGCATCAAGAACTTGACAGGAGCCCAGGCTGACAAGCTGGCCAGC  900
E--C--V--Y--C--K--F--H--F--K--T--N--Q--G--I--K--N--L--T--G--A--Q--A--D--K--L--A--S-
------------------------------------------------------------------------------------
GTGGACCCCGACTACGCCACACGTGATCTGTACAACGCCATCGCCGAGGGCAAGTACCCATCCTGGTCTGTCTTCATACAAGTG  984
V--D--P--D--Y--A--T--R--D--L--Y--N--A--I--A--E--G--K--Y--P--S--W--S--V--F--I--Q--V-
------------------------------------------------------------------------------------
```

ATGAACGTCAAGGATGCTGAGAAGCTCAAGTGGAACCCTTTCGACCTCACCAAGGTGTGGCCCCATGGAGAATACCCCCTCATC 1068

M--N--V--K--D--A--E--K--L--K--W--N--P--F--D--L--T--K--V--W--P--H--G--E--Y--P--L--I-

---

CCTGTTGGTCGCATGGTACTTGACAAGAACCCCAAGAACTACTTTGCTGACGTGGAACAGATCGCCTTCTCCCCGGCGCATATG 1152

P--V--G--R--M--V--L--D--K--N--P--K--N--Y--F--A--D--V--E--Q--I--A--F--S--P--A--H--M-

----------I----------

GTGACAGGTATTGAGGCCAGCCCCGACAAGATGCTGCAGGGTCGCCTCTATTCGTACTCGGACACCCACCGGCATCGTCTCGGC 1236

V--T--*G*--I--E--A--*S*--P--*D*--K--*M--L--Q*--G--*R*--L--Y--S--*Y*--S--*D*--T--H--*R*--H--*R*--L--*G*-

----------Connection domain ----------

AGCAACTACCTGCAACTTCCCGTCAACTGCCCCTACAACACCCGCCTCAGCAACTACCAGAGAGACGGCCCTCAGTGTGTGGAC 1320

S--*N*--Y--L--Q--L--*P--V--N*--C--P--Y--N--T--R--L--S--N--Y--Q--R--D--G--P--Q--C--V--D-

---

AACAACCAAGGTGGCGCTCCTAATTATTTCCCCAACAGTTTCTCCGGCCCCCAAGAGGAATCCAAGTGCATGGAGTGCCCTTTC 1404

N--N--Q--G--G--A--P--N--Y--F--P--N--S--F--S--G--P--Q--E--E--S--K--C--M--E--C--P--F-

---

AAGCTCTCTGGAGACGTCGCCAGATACAGCACAGAGGATGAAGACAACTTCAGCCAAACCGGCATCTTCTGGAAGAAGGTCCTG 1488

K--L--S--G--D--V--A--R--Y--S--T--E--D--E--D--N--F--S--Q--T--G--I--F--W--K--K--V--L-

----------I----------

CCGCCGGGTGAACGGGACCATCTGATCAACAACCTGGCAGGACATATCATCAACGCCCAGGAGTTCATCCAGAAGCGTGCTGTC 1572

P--P--G--E--R--D--H--L--I--N--N--L--A--G--H--I--I--N--A--Q--E--F--I--Q--K--R--A--V-

----------C terminal domain----------

GCCAACTTTGGCAAGGCGGACCCCGAGTTCGGCCGTCGCCTGCAGGCTGCTCTCAACGCCTTGAAAGTGGAGCCATAGATTCGG 1656

A--N--F--G--K--A--D--P--E--F--G--R--R--L--Q--A--A--L--N--A--L--K--V--E--P*

TTGCAGGCAAATCCGGAAGTACAGCCTTGTGTACAGAACAGTCTCCCAGCGTGTATATTGAACTATGCTGACAGATGAATAACT 1740

GATTTGTTACACAGTACACATCGTTGTATTCTGCTTTGCTTTGTATATCGTGTTTAGTTCCACAAATAGCAAGATGGAGAGATT 1824

AATAAGCATACAGTGTAACCATTATGTTTAAAAAGCACTCAAGGAGGCTAAAACGATGAGGGCATATTTTTGAACAGTTACATT 1908

TCTGTTCACGAATGTTTATTAAATTAATGAAAGGCTTTGTTTCTTTGGGAAGGCGCTCCAAGAATGAGTATGTGCAATTATTGA 1992

TCATAAATCTGCGTGAAATTATACTGGAAGGGGAATTTAGCTTAATTTTTGCTATTGTAATAGTATGAGAATTTTCTAGTTCAC 2076

GTTATTTGTATGTGACTTCAACTAAGGTCAGAAATGCAATTAAGCTTAATAAGCGTTCACATTAAAGATAATGTAGCTCTTGTT 2160

AAACCTCTGGACATTTGGTTGAATTACATTTAATATATTGGCAACTATTCAGTGCAAGCGAAGTGCGTCGATCATATCCACTAG 2244

CCCGGCATTATTCTTAAAAGTTGTATTTTACACTCAATGTAAGTATGTTTGGACATAATGTTGATGTTTTGCGTCACACTTCTG 2328

TTATACCTTAGGTGTAACCGAGAAGACAGAATTAAGCCATCAGCTAAAACACTACATACAAGATCAAGGCACAATTGATTTTTT 2412

TTTTTAAATTCTGCCTTGTTTTGTGAAAATATAACATTTATTTCTTGAAAATTTCATGCAACATGAAAACTTGAAAAAAAATCG 2496

AAAATGCAGTGTTTGCATACGCAAGAATGAAAATGTTGGTCAACAGAGTACTATTGTTATATGTTGCCCGTTATTTGCTGCGCT 2580

CTTAATAATCAATACATGGTTGGATAGATATTGATTGAGAAGTAGATGCATGAGCAAGTTCACGTATACAGTGATGCGGAAATT 2664

CCGCATAGAAGCATGTATTCTTCAGCTTATCGCATATTTCATATGGAAATGGGAATTTCACACATTCAATGTACTTAACTGGAT 2748

TCTATAATAATATGTATATTCAATTATTCAAGAGAGGTGATGATAAGACTACAGCTGTAGTGCTACACTTCGGTCCATATTAAG 2832

ATGC**aataaa**ATATTTTGAAAC**AAAAAAAAAA**

Fig. 1: Nucleotide sequence and the deduced amino acid sequence of aCAT. The coding sequence (from 13 to 1515) is in bold letters. Amino acid sequence corresponding to mature protein consists of 501 amino acids. The poly (A) tail is in bold simple case and the polyadenylation signal is indicated by bold capital letters. The neucleotide from 1 to 12 and 1515 to 2720 indicate 5' UTR and 3' UTR respectively. The residues related to heme binding are shaded; those concerned to the NADPH are in bold italics. The residues related to probable catalytic site are boxed. The identified domains are indicated with broken line.

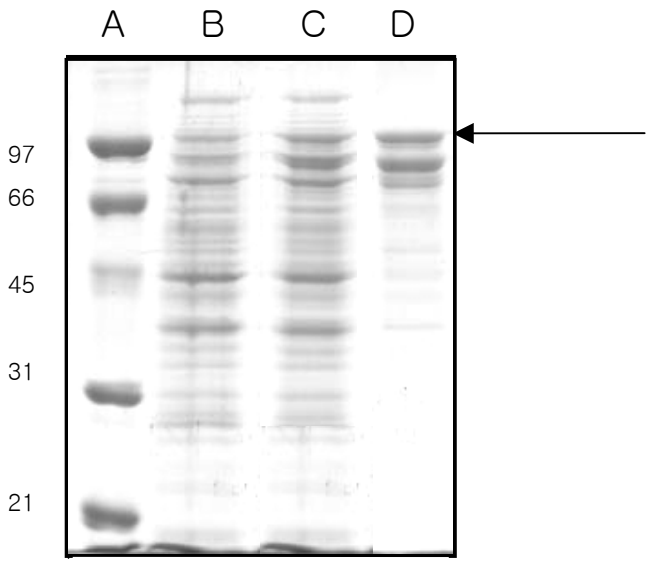

Fig. 2: Analysis of aCAT protein expressed in *E. coli* BL21(DE3) cells following purification in a 12% denaturing polyacrylamide gel. A: Biorad low range protein (precision) standard; B: before induction with IPTG; C: after cells were induced with 1 mM IPTG and grown at 20 ^{o}C for 3 hrs; D: Recombinant protein purified under native conditions by pMAL^{TM} Protein Fusion and purification system

```
human          ---SRDPASDQMQHWKEQRAAQKADVLTTGAGNPVGDKLNVITVGPRGPLLVQDVVFTDE 57
B.taurus       -ADNRDPASDQMKHWKEQRAAQKPDVLTTGGGNPVGDKLNSLTVGPRGPLLVQDVVFTDE 59
X. laevis      MADKRDNAADQMKLWKNGRGSQKPDVLTTGGGNPISDKLNLLTVGPRGPLLVQDVVFTDE 60
D. reiro       MADDREKSTDQMKLWKEGRGSQRPDVLTTGAGVPIGDKLNAMTAGPRGPLLVQDVVFTDE 60
H. discus      -MATRDKASEQLNEFSKGQ--KKPDVLTTGTGAPVGRKTATMTVGPQGPVLLQDFVFTDE 57
L. vannamei    --MPRDKCAEQLNDFKKQQ--TAPDNLTTSHGCPLADKLNSLTVGPRGPILLQDIQLLDE 56
                   *: .::*:: :.: :    .* ***. * *:. *   :*.**:**:*:**. : **

human          MAHFDRERIPERVVHAKGAGAFGYFEVTHDITKYSKAKVFEHIGKKTPIAVRFSTVAGES 117
B.taurus       MAHFDRERIPERVVHAKGAGAFGYFEVTHDITRYSKAKVFEHIGKRTPIAVRFSTVAGES 119
X. laevis      MAHFDRERIPERVVHAKGAGAFGYCEVTHDITKYSKAKVFENIGKRTPIAVRFSTVAGEA 120
D. reiro       MAHFDRERIPERVVHAKGAGAFGYFEVTHDITRYSKAKVFEHVGKTTPIAVRFSTVAGEA 120
H. discus      MAHFNRERIPERVVHAKGAGAFGYLEITHDITKYCKAKVFERVGKKTPLAIRFSTVGGEK 117
L. vannamei    MAHFDRERIPERVVHAKGAGAFGYFEVTHDISKYCKAALFSEIGKRTPIAVRYSTVGGES 116
               ****:****************** *:****::*.** :*..:** **:*:*:***.**

human          GSADTVRDPRGFAVKFYTEDGNWDLVGNNTPIFFIRDPILFPSFIHSQKRNPQTHLKDPD 177
B.taurus       GSADTVRDPRGFAVKFYTEDGNWDLVGNNTPIFFIRDALLFPSFIHSQKRNPQTHLKDPD 179
X. laevis      GSSDTVRDPRGFAVKMYTEDGNWDLTGNNTPVFFIRDAMLFPSFIHSQKRNPQTHLKDPD 180
D. reiro       GSSDTVRDPRGFAVKFYTDEGNWDLTGNNTPIFFIRDTLLFPSFIHSQKRNPQTHLKDPD 180
H. discus      GSADTARDPPGVRHKFYTEDGNWDLVGNNTPIFFIRDPMLFPSFIHTQKRNPVTNLKDPD 177
L. vannamei    GSTDTARDPRGFAVKFYTEEGNWDLVGNNTPIFFIRDPILFPSFIHTQKRNPATHLKDCD 176
               **:**.*** *.  *:**::*****.*****:*****.:*******:***** *:*** *

human          MVWDFWSLRPESLHQVSFLFSDRGIPDGHRHMNGYGSHTFKLVNANGEAVYCKFHYKTDQ 237
B.taurus       MVWDFWSLRPESLHQVSFLFSDRGIPDGHRHMDGYGSHTFKLVNADGEAVYCKFHYKTDQ 239
X. laevis      MVWDFWSLRPESLHQVSFLFSDRGIPDGHRHMNGYGSHTFKLVNAKDEAVYCKFHYKTDQ 240
D. reiro       MVWDFWSLRPESLHQVSFLFSDRGIPDGYRHMNGYGSHTFKLVNAQGQPVYCKFHYKTNQ 240
H. discus      MFWDFITLRPETTHQVAFLFSNRGTPDGYRHMNGYGSHTFKMVNAKGECVYCKFHFKTNQ 237
L. vannamei    MFWDFISLRPETTHQVSFLFSDRGTPDGYRHMNGYGSRTSKLVNEKGEAVYCKFHYKTDQ 236
               *.*** :****: ***:****:** ***:***:****:* *:** ..: ******:**:*

human          GIKNLSVEDAARLSQEDPDYGIRDLFNAIATGKYPSWTFYIQVMTFNQAETFPFNPFDLT 297
B.taurus       GIKNLSVEDAARLAHEDPDYGLRDLFNAIATGNYPSWTLYIQVMTFSEAEIFPFNPFDLT 299
X. laevis      CIQNLTVDEANRLAASDPDYGIHDLYEAITTGNYPSWSFYIQVMTFEQAERFKFNPFDLT 300
```

```
D. reiro        GIKNIPVEEADRLAATDPDYSIRDLYNAIANGNFPSWTFYIQVMTFEQAENWKWNPFDLT 300
H. discus       GIKNLTGAQADKLASVDPDYATRDLYNAIAEGKYPSWSVFIQVMNVKDAEKLKWNPFDLT 297
L. vannamei     GIKCLSSKKADELAGSDPDYATRDLYNAISSGDYPSYTMCIQVMTFEEAEKWKFNPFDLT 296
                 *: :.  .* .*:  ****. :**::**: *.:**::. ****...:**   :******

human           KVWPHKDYPLIPVGKLVLNRNPVNYFAEVEQIAFDPSNMPPGIEASPDKMLQGRLFAYPD 357
B.taurus        KVWPHGDYPLIPVGKLVLNRNPVNYFAEVEQLAFDPSNMPPGIEPSPDKMLQGRLFAYPD 359
X. laevis       KIWPHGDYPLIPVGKLVLNRNPTNYFAEVEQLAFDPSNMPPGIEPSPDKMLQGRLFSYPD 360
D. reiro        KVWSHKEFPLIPVGRFVLNRNPVNYFAEVEQLAFDPSNMPPGIEPSPDKMLQGRLFSYPD 360
H. discus       KVWPHGEYPLIPVGRMVLDKNPKNYFADVEQIAFSPAHMVTGIEASPDKMLQGRLYSYSD 357
L. vannamei     KVWPHGEFPLIPVGRLTFDRNPKNYFAEVEQIAFSSANMVPGIEASPDKMLQGRLFSYND 356
                 *:*.* ::******::.:::** ****:***:**..::* .***.**********::* *

human           THRHRLGPNYLHIPVNCPYRARVANYQRDGPMCMQDNQGGAPNYYPNSFGAPEQQPSALE 417
B.taurus        THRHRLGPNYLQIPVNCPYRARVANYQRDGPMCMMDNQGGAPNYYPNSFSAPEHQPSALE 419
X. laevis       THRHRLGPNYLQLPVNCPYRTRVANYQRDRPMCFTDNQGGAPNYYPNSFCAPENQPQVRE 420
D. reiro        THRHRLGANYLQLPVNCPYRTRVANYQRDGPMCMHDNQGGAPNYYPNSFSAPDVQPRFLE 420
H. discus       THRHRLGSNYLQLPVNCPYNTRLSNYQRDGPQCVDNNQGGAPNYFPNSFSGPQEESKCME 417
L. vannamei     THRHRLGANYTQIPVNCPYRARTRNYQRDGPMCVDGNQESAPNYFPNSFSGPQDCRKHTA 416
                 *******.** ::******.:*  ***** * *. .** .****:**** .*:

human           HSIQYSGEVRRFNTANDDNVTQVRAFYVNVLNEEQRKRLCENIAGHLKDAQIFIQKKAVK 477
B.taurus        HRTHFSGDVQRFNSANDDNVTQVRTFYLKVLNEEQRKRLCENIAGHLKDAQLFIQKKAVK 479
X. laevis       HRFQVSADVARYNSSDEDNVSQVRDFYVKVLSEEQRLRLCENIAGHLKDAQLFIQKRAVK 480
D. reiro        SKCKVSPDVARYNSADDDNVTQVRTFFTQVLNEAERERLCQNMAGHLKGAQLFIQKRMVQ 480
H. discus       CPFKLSGDVARYSTEDEDNFSQTGIFWKKVLPPGERDHLINNLAGHIINAQEFIQKRAVA 477
L. vannamei     PKFSVSADVDRYNSADEDNFTQVGIFYRQVLNEAERQRLVENIAGHMVGAQEFIQDRAIK 476
                      * :* *:.: ::**.:*.  *: :**   :* :* :*:***: .** ***.: :

human           NFTEVHPDYGSHIQALLDKYN---------------------------- 498
B.taurus        NFSDVHPEYGSRIQALLDKYNEEKPKN---------------------- 506
X. laevis       NFTDVHPEYGARIQALLDKYNAEGAKKKTVKTYTQHSSYATSKDKANL 528
D. reiro        NLMAVHSDYGNRVQALLDKHNAEGKKN-TVHVYSRGGASAVAAASKM- 526
H. discus       NFGKADPEFGRRLQAALNALKVEP------------------------ 501
L. vannamei     NFTQADPEYGANIRRAIDKIKMSQASSKT------------------- 505
```

: ...:: .:: :: :

Fig. 3: Multiple sequence alignments of (human, human erythrocyte; *B. taurus*, cow; *X. laevis,* African clawed frog; *D. rerio,* zebrafish and *L. vannamei,* pacific white shrimp) known catalase amino acid sequences. The alignment program Clustal W automatically introduces gaps (dash) to maximize similarity among the primary structures of these catalases. All amino acid residues identical to corresponding ones of aCAT are represented with asterisks. Conserved substitutions depending on functionality are indicated with colon and the semi-conserved residues with a dot. The putative catalytic site is marked with a box.

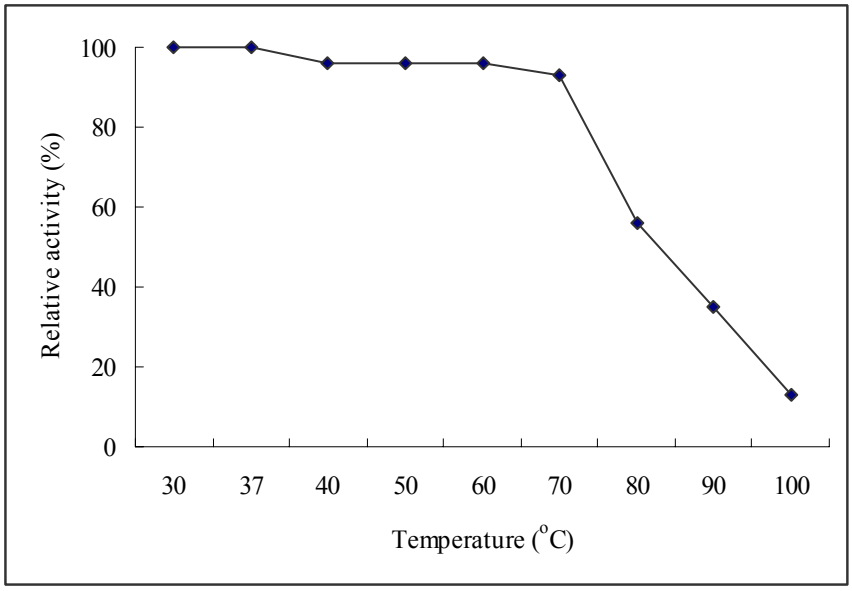

Fig. 4: Optimal temperature of aCAT. Enzyme activity was carried out at different temperatures (30, 37, 40, 50, 60, 70, 80, 90 and 100 °C) and relative activity was determined.

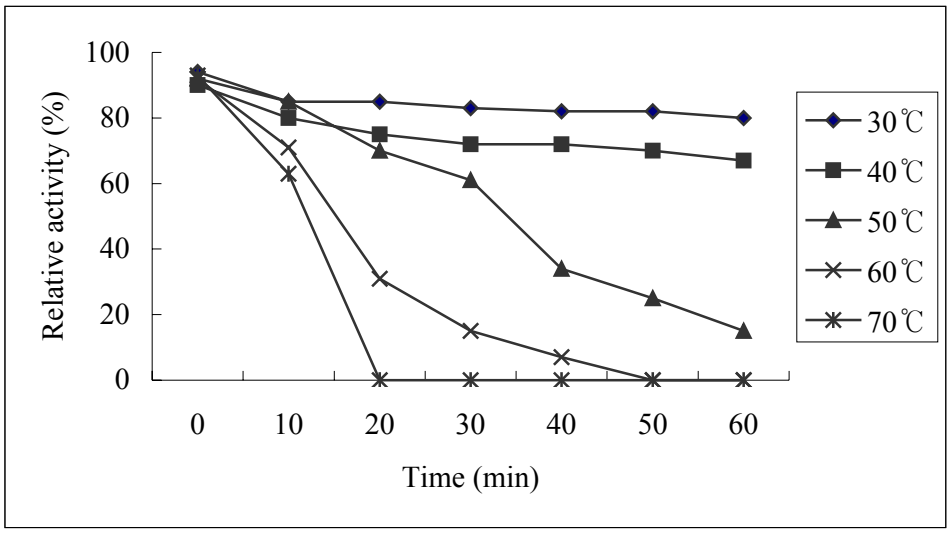

Fig. 5: Thermal stability of aCAT. Enzyme stability at different temperatures was assessed by heating aliquots of aCAT at 30, 40, 50, 60 and 70 ^{o}C for 0, 10, 20, 30, 40, 50 and 60 mins. The residual enzyme activity was determined

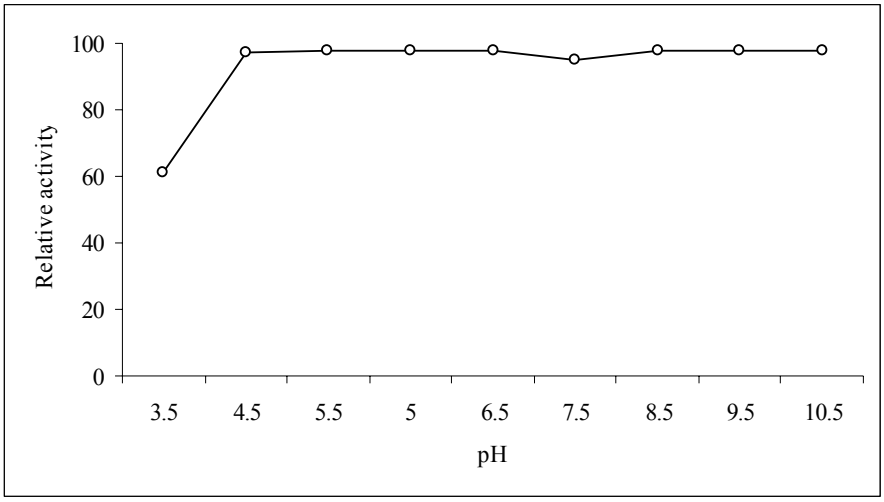

Fig. 6: Optimal pH of aCAT. The enzyme activity was carried out in buffers with different pH values and relative activity was determined.

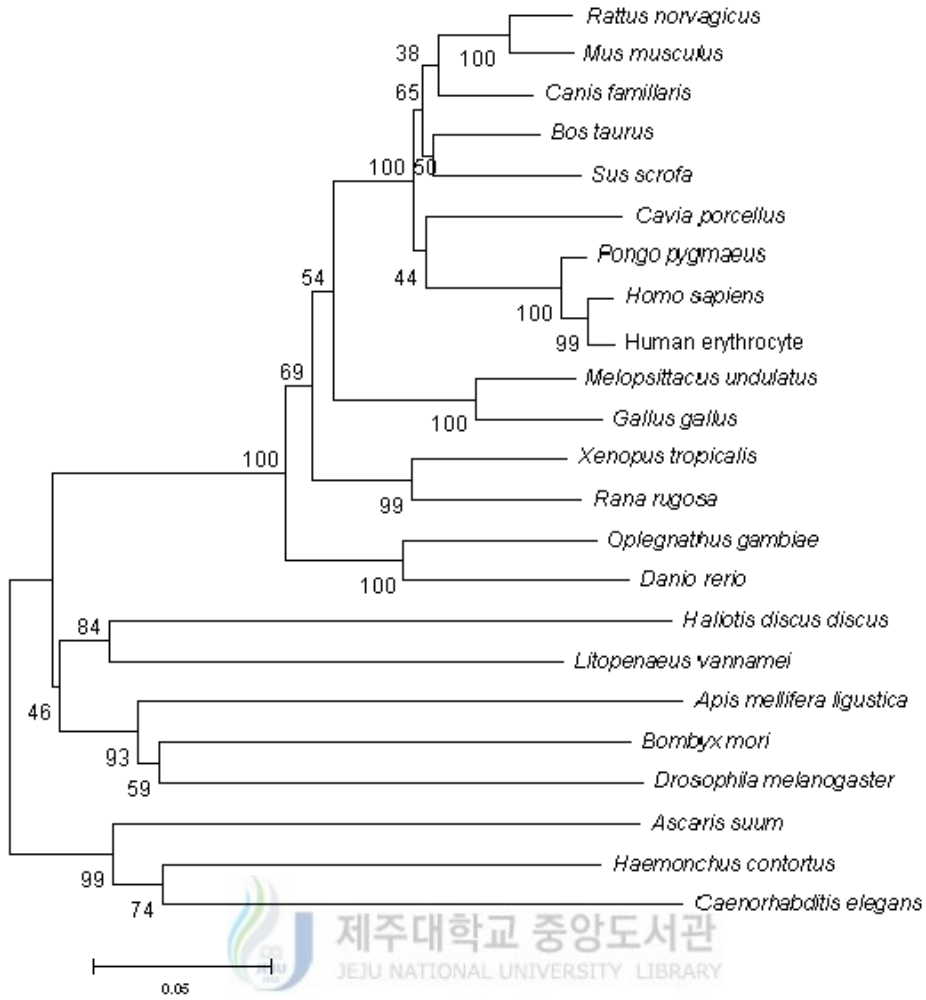

Fig. 7: Neighbor-joining tree based on catalase amino acid sequences obtained from 23 species. (MEGA 3.0, Kumar et al., 2004). Bootstrap values (1000 replications) are displayed over internal nodes.

4. DISCUSSION

Cloning and analysis of aCAT:

In this study, we present evidence for the cloning of a gene encoding catalase (aCAT) from *H. discus discus* digestive gland cDNA. Many studies have been already carried out on cloning and characterization of catalases from different species (Thuy et al., 2004; Hass et al., 1991; Ni et al., 2001; Nakamura et al., 2000; Moreira et al., 2004; Kwon and An, 2001). Some studies have also been carried out to assess the importance of catalase in the antioxidant defense system by over expressing catalase in cell lines and transgenic mice (Chen et al., 2004). Cloning and sequencing of the aCAT cDNA revealed a coding region of 1503 nucleotides and 12 bp 5' untranslated region and 1216 bp 3' untranslated region (Fig.1).

Comparison of deduced amino acid sequence of aCAT with 22 known catalases by CLUSTAL W (1.82) multiple sequence alignment program revealed that 173 amino acid residues conserved in all 22 species. This accounts to 34.5% similarity at amino acid level. The alignment of aCAT with catalases from human erythrocyte, *Bos Taurus* (cow), *Xenopus laevis* (african clawed frog), *Danio rerio* (zebrafish) and *Litopenaeus vannamei* (pacific white shrimp) is shown in Fig. 3. The Comparison of aCAT with above 5 sequences revealed that 264 amino acid residues were conserved in all catalases accounting for 52.69% identity at amino acid level. Since the number of residues in the nucleotide sequence is 3 times higher than the amino acid sequence it codes, the nucleotide sequence may hold 3

times more mutations than that of the amino acid sequence, while maintaining the same conservation. Zamocky and Koller (1999) reported that a so-called consensus sequence contains 84 residues highly conserved in many catalases. The alignment reveals that aCAT shares about 66, 65, 66, 69, and 65% identity with human erythrocyte, *B. taurus*, *X. laevis*, *D. rerio* and *L. vannamei* catalases respectively. Moreover, aCAT also contained the conserved H_{72}, present in all heme catalases (Fig. 3). This residue has been reported to allow the proper binding and reduction of a peroxide molecule (Thuy et al., 2004). According to the Moreira et al. (2004), the catalytic site is composed of amino acids F-D-R-E-R-I-P-E-R-V-V-H-A-K-G-A and G, which is conserved in aCAT at positions 61-79 in the amino acid sequence. Moreover, this active site is conserved in all other five catalase sequences we considered in Fig. 3. NADPH is reported to be tightly bound to several catalases, although the role of the dinucleotide remains unclear (Fita and Rossmann, 1985). In this study, we identified 29 amino acid residues responsible for binding of the NADPH. Eight of them were also conserved in the sequence of human erythrocyte CAT which the structure was recently determined (Yamamoto et al., 2005). Studies on the role of NADPH in the BLC suggests that NADPH could be both preventing and reversing the accumulation of intermediate compound (known as compound II) in the catalytic action (Kirkman et al., 1987). Experiments with *Saccharomyces cerevisiae* catalase-A proposed that in addition to its role in the recycling

mechanism, binding of NADPH stabilizes the quaternary structure of the protein (Zamocky and Koller, 1999).

Fita and Rossmann (1985) have determined the three-dimensional crystal structure of the mammalian catalase for BLC. The deduced amino acid sequence of aCAT shows 65% of identity with that of BLC allowing us to suggest that the three dimensional structure of aCAT be similar to that of BLC. Further, the amino acid residues interacting with heme and NDPH are highly conserved in both sequences.

Overexpression of aCAT in *E. coli* BL 21 DE3:

Cloning of coding sequence to pMAL-c2X plasmid resulted in expression of soluble aCAT when induced with IPTG in *E. coli* BL 21(DE3) cells. According to structural and functional similarities, catalases can be divided into three subgroups namely typical (true catalases), catalase peroxidase and manganese catalase or non-heme catalase (Zamocky and Koller, 1999). The catalase identified from abalone gonad cDNA in this study belongs to typical catalase. The largest subgroup; typical catalases are homotetrameric heme proteins varying the molecular weight from 200- 340 kDa. In agreement, the aCAT isolated, coded for 501 amino acid expecting a size of 56 kDa with a pI of 8.8 pH, containing lysine and glycine as the major constituents (Expert Protein Analysis System, proteomics server from the Swiss Institute of Bioinformatics). Fig. 2 confirms the expected size of the protein as 98 kDa together with the fusion protein where maltose binding protein (MBP) contributes to 42 kDa molecular weight. When

aCAT was expressed in *E. coli* BL21(DE3) cells, and analysed on 12% SDS-PAGE, a distinct band could be observed after induction with IPTG and purification with amylose resin column compared to the samples uninduced (Fig. 2). The reason for the other two bands present after the purification could be due to the degradation of the MPB-aCAT fusion protein. Western blotting using mono-clonal antibody against MBP confirmed that the other two bands are MBP-aCAT variants (data not shown). Thuy et al. (2004) reported that for most industrial applications, especially in the textile industry, bovine liver catalase (BLC) is used. The overexpressed of aCAT in *E. coli* suggests the possibility of using this system as a source of catalase in industrial work. Since the purified catalase showed 30,000 U/mg activities both with and without cleaving the fusion protein with factor Xa (data not shown), protein without cleaving was used for further experiment in this study.

Optimal temperature and thermal stability:

The rate at which an enzyme works is influenced by several factors including the temperature. It is important to determine an optimal temperature for enzymatic action. The Fig. 4 demonstrates that aCAT was active following exposure up to 70 ^{o}C and then decrease the activity. The higher thermal stability is probably due to its long β- barrel domain containing the catalytic site with hem moiety. Some catalases reported to have elongated C-terminal domains, which contribute to increase stability against chemicals and under high temperature. *Penicillium vitale* typical

catalase and HPII from *E. coli* reported to contain such domains with a "falvodxin-like" topology (Zamocky and Koller, 1999). Studies on BLC – structure revealed that it includes a β-barrel, which consists of two four stranded anti-parallel β-sheets that twist to form a closed cylindrical surface making the heat inactivation of BLC at higher temperature a difficult task. Thuy et al. (2004) suggest that thermo-stability of catalase from *Halomonas* sp. SK1 overexpressed in *E. coli* is due to elongated C-terminal peptide. Contrasting study is reported by Nakano et al. (1995) where catalase from seaweed *Porphyra yezoensis* had activity only up to 50 ^{o}C.

The thermal stability of aCAT is shown in Fig 5. It can be observed that irreversible thermal inactivation occurred when heating the protein at 50, 60 and 70 ^{o}C for about 30 mins. On the other hand heat inactivation was not observed when heated at 30 and 40 ^{o}C even for 1 hr. Observed thermal stability at 30 and 40 ^{o}C could be a result of the fusion protein or due to its nature.

Optimal pH:

In agreement with the studies conducted by Hass et al. (1991), where recombinant catalase from *Listeria seeligeri* showed activity in a broad spectrum of pH, aCAT was also active in a wide range of pH (Fig. 6) making the overexpressed protein in this study easy to use in the industry. Mostly the industrial wastes are alkaline, specially in the textile industry where commercial catalases are highly used. In this case, aCAT cloned in a bacterium that survives under extreme conditions may be a suitable

replacement as it shows high activity in a broad range of pH. When characterizing catalase from *Porphyra yezoensis,* Nakano et al. (1995) have also observed the high activity of catalase from the seaweed over a very wide pH range (6.0-11.0). However, they have observed decrease in activity below pH 6.0 where we observed the decrement below pH 4.5. The reason could be due to the former is from plant and latter from animal source.

Phylogenetic analysis:

Catalase, primarily responsible for the metabolism of hydrogen peroxide, is a key antioxidant enzyme that is present throughout phylogeny, from bacteria to humans. BLAST program (Basic Local Alignment Search Tool), was used to search for all complete protein sequences of catalases. Twenty-two eukaryote sequences were considered to visualize the relationship between aCAT in terms of amino acid sequence similarity and phylogenetic tree was constructed. Fig. 7 shows the deduced phylogeny of aCAT, as calculated from neighbor-joining tree based analysis on amino acid sequences. The aCAT sequence was closer to pacific white shrimp revealing 84% boot-strap value.

Oxidative stress has been defined as “a disturbance in the pro-oxidant-antioxidant balance” in favor of the former, leading to potential damage (Kaizer et al., 2005). Physiological responses to oxidative stress in mammals have been studied by many researchers (Thuy et al., 2004; Bouzyk et al., 2000). Shull et al. (1991) reported that catalase mRNA is induced by oxidative stress in lung epithelial cells. Even though it was not

considered studying about the role of catalase in abalone in this study, most probably aCAT is playing a crucial role in healing the oxidative stress by facilitating the degradation of H_2O_2. Further research should be carried out to study the role of aCAT in the abalone's internal defense system.

In conclusion, gene encoding the abalone (*H. discus discus*) catalase was sequenced, and the recombinant aCAT was successfully overexpressed in *E.coli* BL23(DE3) cells and characterized for the first time. This enzyme suggestively belonged to typical catalase can be used in the industry as well as the information on the aCAT sequence can be used in comparative studies on marine invertibrate catalases which are just flourishing to be investigated.

Part II

Molecular cloning, expression, purification and characterization of Cu,Zn-superoxide dismutase from Abalone, *Haliotis discus discus* cDNA

1. ABSTRACT

Cu,Zn-superoxide dismutase (Cu,Zn-SOD) is a metalloenzyme that catalyzes dismutation of harmful superoxide radicals into H_2O_2 and O_2. This work reports the sequencing, cloning, expression and characterizing of Cu,Zn-superoxide dismutase (aCu,Zn-SOD) encoding gene from the disk-abalone (*Haliotis discus discus*) cDNA library. The full-length cDNA contained 1027 bp, with an ORF of 465 bp coding for 154 amino acids with a pI value of 5.5. The expression of gene in *E.coli* K12 (TB1) resulted in a soluble protein of 16 kDa. The purified protein exhibited 2461 Unit/mg activity when induced with 0.5 mM of IPTG. The optimum temperature of the enzyme was 37 ^{o}C and it was active in a range of acidic pH (from 3.5 to 6.5). The enzyme was heat inactivated after 70 ^{o}C. When compared with 47 other Cu,Zn-SODs, it was revealed that 48 amino acid residues were conserved in all 47 species, accounting for 29% identity. In comparison with known Cu,Zn-SODs, where structural studies have been carried out, the residues maintaining the active site geometry were conserved in aCu,Zn-SOD amino acid sequence (Gly45, Gly62, Pro75 and Gly83). Findings of this study will contribute more to the future studies of comparative genomics on invertebrate Cu,Zn-SOD.

2. MATERIALS AND METHODS

Cloning and sequencing of the gene encoding aCu,Zn-SOD:

A clone with an expected function of Cu,Zn-SOD was selected from the abalone cDNA library. The plasmid DNA of the putative aCu,Zn-SOD was isolated by the Accuprep^{TM} plasmid extraction kit (Bioneer Co., Korea). The full-length sequence was determined by sequencing reactions from 3' end using oligo dT primer. After deriving the full length, the sequence was compared with the Cu,Zn-SOD sequences in the database of the National Center for Biotechnology Information (NCBI), BLAST-X.

Cloning the coding sequence of aCu,Zn-SOD into the pMAL expression vector:

Having checked the restriction enzyme sites of the aCu,Zn-SOD sequence, a pair of primers was designed for cloning the coding sequence of the aCu,Zn-SOD into the expression vector, pMAL-c2X (New England Biolabs, USA). The sense amplification primer was designed as 5'-gagagaGAATTCATGTCTATCAAAGCAGTTTGTGTGC -3' having *Eco*R I site and antisense primer 5'-gagagaAAGCTTTCACTTGGTGATGCCGATCA -3' containing *Hind* III site. In a total of 50 µl of PCR reaction, 5 units of Ex Taq polymerase (Takara Korea Biomedical Inc., Korea), 5 µl of 10X Ex Taq buffer, 4 µl of 2.5 mM dNTP, 50 ng of template and 50 pmol of each primer were used. After initial incubation at 94 ^{o}C for 2 min, 25 cycles were carried out with 30 sec denaturation at 94 ^{o}C, 30 sec of annealing at 55 ^{o}C, and 30 sec of

elongation at 72 ^{o}C, followed by a final extension at 72 ^{o}C for 5 min. The PCR product was analysed using 1% agarose gel and ethidium bromide staining. Thereafter it was purified by the Accuprep^{TM} gel purification kit (Bioneer Co., Korea) and digested with *Eco* RI and *Hind* III restriction enzymes. The expression vector, pMAL-c2X, was digested with the same restriction enzymes as the PCR product and dephosphorylated with calf intestine phosphatase (NEB, USA) according to the vendor's protocol. Thereafter the vector and the PCR product was purified by a 1% agarose gel using the Qiaex-II gel purification kit (QIAGEN Inc., USA).

Ligation was carried out at 16 ^{o}C, overnight with 100 ng of pMAL-c2X vector, 70 ng of PCR product, 1 µl of 10X ligation buffer and 0.5 µl 1X T4DNA ligase (Takara Korea Biochemical Inc., Korea). The ligated product was transformed into XL1 cells. The correct recombinant (confirmed by colony cracking, restriction enzyme digestion and sequencing), was transformed into competent cells *E. coli* K12 (TB1).

Overexpression of aCu,Zn-SOD:

The recombinant enzyme was overexpressed in *E coli* K12(TB1) cells in the presence of isopropyl-ß-thiogalactopyranoside (IPTG). A volume of 10 ml of starter culture was inoculated into 100 ml Luria broth with 100 µl ampicillin (100 mg/ml) and 10 mM glucose (2% final concentration) and kept at 37 ^{o}C with 200 rpm until OD_{600} approached 0.5.The culture was then shifted to 20 ^{o}C for 15 min prior to the induction with 0.5 mM IPTG at the final concentration. After 3 hrs of induction, the cells were cooled on ice for

30 min and harvested by centrifugation at 4000 rpm for 20 min at 4 ^{o}C. The cells were re-suspended with 5 ml column buffer (Tri-HCl, pH 7.4 + NaCl) and freezed in –70 ^{o}C.

Purification of aCu,Zn-SOD :

After thawing, the bacterial cells were placed in an ice-water bath and sonicated six times in short pulses of 10 sec. Having centrifuged at 9000 x g for 30 min at 4 ^{o}C, the supernatant was diluted with a 1:5 column buffer. The pMAL^{TM} protein fusion and purification system was followed. In brief, amylose resin was poured into a 1 x 5 cm column and washed with 8 x column volumes of column buffer. The diluted crude extract was loaded at a flow rate of 1 ml/hr. The column was then washed with 12 x column volumes of column buffer and the fusion protein was eluted with elution buffer (column buffer + 10 mM maltose). The elute was collected in 500 μl fractions. The eluted protein content was measured by UV absorbance at 280 nm. A slight modification was done to the column buffer by excluding EDTA as SOD disassociates with EDTA. Discontinuous SDS-PAGE was performed according to its standard procedure. The stacking and separating gels were prepared at 5 and 12% respectively and the gel was stained with Coomassie blue.

Cu,Zn-SOD activity assay and determination of protein concentration:

Activity of aCu,Zn-SOD was detrmined by the xanthine oxidase method according to the procedures described by Nagai et al. (2003). The reaction mixture consisted of 0.48 ml of 0.05 M sodium carbonate buffer (pH

10.5), 0.02 ml of 3 mM xanthine, 0.02 ml of 3 mM EDTA, 0.02 ml of 0.15% bovine serum albumin, 0.02 ml of 0.75 mM NBT and 0.02 ml of aCu,Zn-SODsample. After incubation at 25 °C for 10 minutes, the reaction was initiated by adding 6 mU xanthine oxidase and maintaining the temperature at 25 °C for 20 min. The reaction was stopped by adding 0.02 ml of 6 mM $CuCl_2$. The absorbance was recorded in a microplate reader (Sunrise; Tecan Co. Ltd., Austria) at 560 nm. One Unit was defined as the amount of enzyme required to reduce the reaction by 50%. Specific activity was defined as Unit/mg protein. The protein concentration was determined by the procedure of Lowrey et al. (1951) using bovine serum albumin as the standard.

In order to determine the optimal temperature, each reaction was carried out at 25, 30, 37, 40, 50, 60, 70 and 80 ^{o}C and the relative activity was determined. To determine the optimal pH of the aCu,Zn-SOD each reaction was carried out in acetate buffer pH 3.5 - 5.5, phosphate buffer pH 6.5 - 7.5 and glycine-NaOH buffer pH 8.5 - 10.5 and the relative activity was determined.

Analysis of nucleotide and amino acid sequences:

Nucleotide sequence analysis was performed with the DNAssit program (version 2.2). The NCBI BLAST program (http://www.ncbi.nlm.nih.gov) was used to search for nucleotide and protein sequences homologous to the aCu,Zn-SOD. The protein sequences were aligned with the CLUSTAL W multiple sequence alignment program (version 1.8). Phylogenetic relationship was determined by reconstructing a protein phylogeny using

MEGA3.1 program (Kumar et al., 2004). Neighbor-Joining algorithm with the PAM matrix model was applied in constructing in the phylogenetic tree. The tree topology was evaluated by the bootstrapping method (1000 replications).

3. RESULTS

GGGGATTACAGTGCAATTTCTCGGCGGTCTCGGCTACAACAAGCACTTTCCGGTGAAATATTCAGCTCTTGAAAC 75

ATGTCTATCAAAGCAGTTTGTGTGCTGAGAGGTGATTCGGAAGTCAAGGGAACAGTATTCTTCTCACAGGGAGATGCAGAC 156

M--S--I--K--A--V--C--V--L--R--G--D--S--E--V--K--G--T--V--F--F--S--Q--G--D--A--D-

AGTCCAGTGAAAGTGACGGGCTCCATCACGGGCCTGACGGAGGGCAAACATGGCTTCCACGTTCATCAGTTCGGGGACAAC 237

-S--P--V--K--V--T--G--S--I--T--G--L--T--E--G--K--H--G--F--H--V--H--Q--F--G--D--N

ACGAATGGCTGTACCAGTGCCGGGTCCCACTTCAACCCTTTCGGCAAGACCCATGGAGCGCCAGAAGACGAAAACAGACAT 319

--T--N--G--C--T--S--A--G--S--H--F--N--P--F--G--K--T--H--G--A--P--E--D--E--N--R--

GCTGGTGACCTTGGCAACGTTACTGCTGACGCATCAGGAGTAGCAAACATCGACATCGAGGACAAGATCATAAGTTTGACT 399

H--A--G--D--L--G--N--V--T--A--D--A--S--G--V--A--N--I--D--I--E--D--K--I--I--S--L-

GGGGACAAATCAATCATTGGCAGAACTATTGTTGTCCATGCTGGAGTGGATGACCTGGGCAAGGGAGGCAATGAAGAAAGC 480

-T--G--D--K--S--I--I--G--R--T--I--V--V--H--A--G--V--D--D--L--G--K--G--G--N--E--E

CTGAAGACAGGGAACGCTGGTGGTCGTCAGGCCTGTGGGGTGATCGGCATCACCAAGTGACCAAAGTGTTGAATCAGTTGC 561

--S--L--K--T--G--N--A--G--G--R--Q--A--C--G--V--I--G--I--T--K--

GTCAGCACCATGTGGTGTCTTACCGCTAGCATAGGTGGGAATTTGTTGTACCAGATGAAGTTTATTTGTTGTTTGTTGGG 641

CATTATTGCAAAATAACTATTCCAAACGTTAACTTTTTTTCAAATTGTGGACGTTTCATGTAGAAAATAAATCTATGGAA 721

AATAAGACTGACAAGCCATTTTCTAATTCATAAGTTGGAGGGTTTTTTTTGTTCAGCTGAACTACCGGTAGAATATTTGT 901

GTTTAATATGCTCTAGGTCAGACACGTTACTCTTCATTCCAAGACTATCTAGACTGATTGTATATCCCTGAGCTAGCTAT 992

TTGCTGTTGAATCATTGATACTGGAATTCCATAATGTGGAACAATGTTGCACCTTTTGGTGTGGGGTGATCACTGTCTATC 962

TAAGAGTACAAAGAG**aataaa**TCCTACTGTTGTAT***AAAAAAAAAAAAAAAAAAAAAAAAAA*** 1025

Fig. 8: Nucleotide sequence and the deduced amino acid sequence of aCu,Zn-SOD. The coding sequence (from 76 to 537) is in bold letters. Amino acid sequence corresponding to protein consists of 154 amino acids. The poly (A) tail is in bold italics and the polyadenylation signal is indicated by bold simple case. The neucleotide from 1 to 75 and 538 to 999 indicate 5' UTR and 3' UTR respectively. The residues that interact with copper and zinc are underlined and boxed respectively. Five well conserved active sites are shaded.

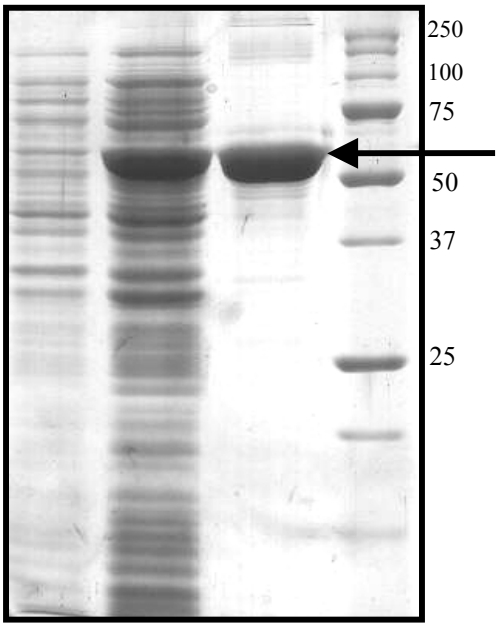

Fig. 9: Analysis of aCu,Zn-SOD protein expressed in *E. coli* K12(TB1) cells following purification in a 12% denaturing polyacrylamide gel. Cells were grown at 30 ^{o}C and induced with 0.5 mM IPTG. Recombinant protein was purified under native conditions by pMAL^{TM} Protein Fusion and purification system.

```
S. scrofa        -AT-KAVCVLKGDGPVQGTIYFELKGEK-TVLVTGTIKGLAEGDHGFHVHQFGDNTQGCT 57
B. taurus        MAT-KAVCVLKGDGPVQGTIHFEAKGD--TVVVTGSITGLTEGDHGFHVHQFGDNTQGCT 57
H. sapiens       MAT-KAVCVLKGDGPVQGIINFEQKESNGPVKVWGSIKGLTEGLHGFHVHEFGDNTAGCT 59
G. gallus        MATLKAVCVMKGDAPVEGVIHFQQQGSG-PVKVTGKITGLSDGDHGFHVHEFGDNTNGCT 59
H. discus        -MSIKAVCVLRGDSEVKGTVFFSQGDADSPVKVTGSITGLTEGKHGFHVHQFGDNTNGCT 59
H. diversicolor -MSVKAVCVLKGAGEVEGTIHFSQTEADGPVTVTGKISGLEGGLHGFHVHEFGDATNGCM 59
                  : *****::* . *:* : *.     ..* * *.*.**  * ******:*** * **

S. scrofa        SAGPHFNPESKKHGGPKDQERHVGDLGNVTAGKDGVATVYIEDSVIALSGDHSIIGRTMV 117
B. Taurus        SAGPHFNPLSKKHGGPKDEERHVGDLGNVTADKNGVAIVDIVDPLISLSGEYSIIGRTMV 117
H. sapiens       SAGPHFNPLSRKHGGPKDEERHVGDLGNVTADKDGVADVSIEDSVISLSGDHCIIGRTLV 119
G. gallus        SAGAHFNPEGKQHGGPKDADRHVGDLGNVTA-KGGVAEVEIEDSVISLTGPHCIIGRTMV 118
H. discus        SAGSHFNPFGKTHGAPEDENRHAGDLGNVTADASGVANIDIEDKIISLTGDKSIIGRTIV 119
H. diversicolor SAGPHYNPFGKTHGAPEDENRHAGDLGNVLANADGVADIKIDDRIISLTGVRSIIGRTIV 119
                ***.*:** .: **.*:* :**.****** *. .*** : * * :*:*:*  .*****:*

S. scrofa        VHEKPDDLGRGGNEESTKTGNAGSRLACGVIGITQ- 152
B. Taurus        VHEKPDDLGRGGNEESTKTGNAGSRLACGVIGIAK- 152
H. sapiens       VHEKADDLGKGGNEESTKTGNAGSRLACGVIGIAQ- 154
G. gallus        VHAKSDDLGRGGDNESKLTGNAGPRLACGVIGIAKC 154
H. discus        VHAGVDDLGKGGNEESLKTGNAGGRQACGVIGITK- 154
H. diversicolor VHAGKDDLGKGGNEESLKTGNAGGRLACGVVGITK- 154
                **   ****:**::**  ***** * ****:**::
```


Fig. 10: Sequence comparison of aCu,Zn-SOD with *S. scrofa* (P04178), *B. taurus,* (P00442), *H. sapiens* (P00441), *G. gallus* (NP990395) and *H. diversicolor supertext* (AAY18806). The alignment program Clustal W automatically introduces gaps (dash) to maximize similarity among the primary structures of these Cu,Zn-SODs. All amino acid residues identical to corresponding ones of *H. discus discus* are represented with asterisk.

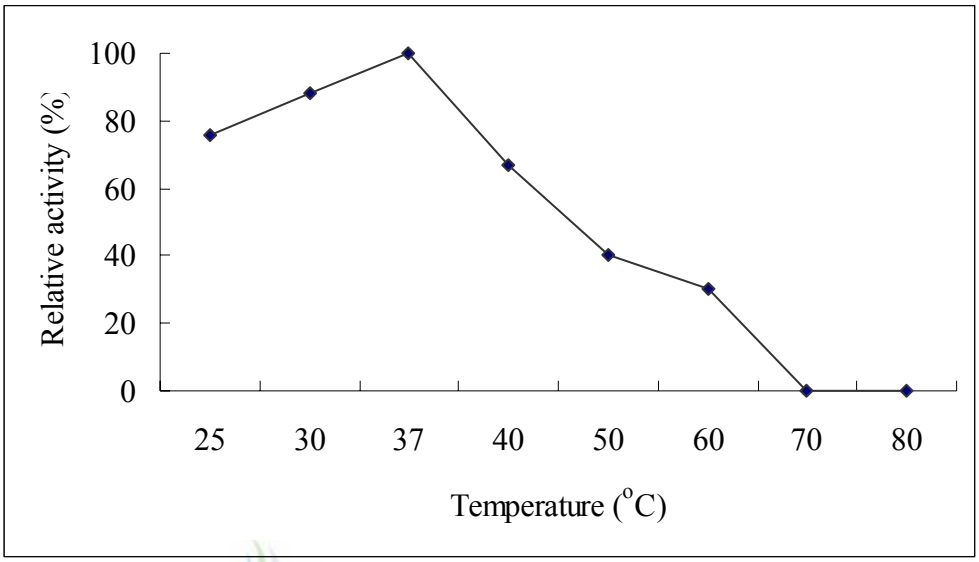

Fig. 11: Optimal temperature of aCu,Zn-SOD. Enzyme activity was carried out at different temperatures (25, 30, 37, 40, 50, 60, 70 and 80 °C) and relative activity was determined by xanthine oxidase method.

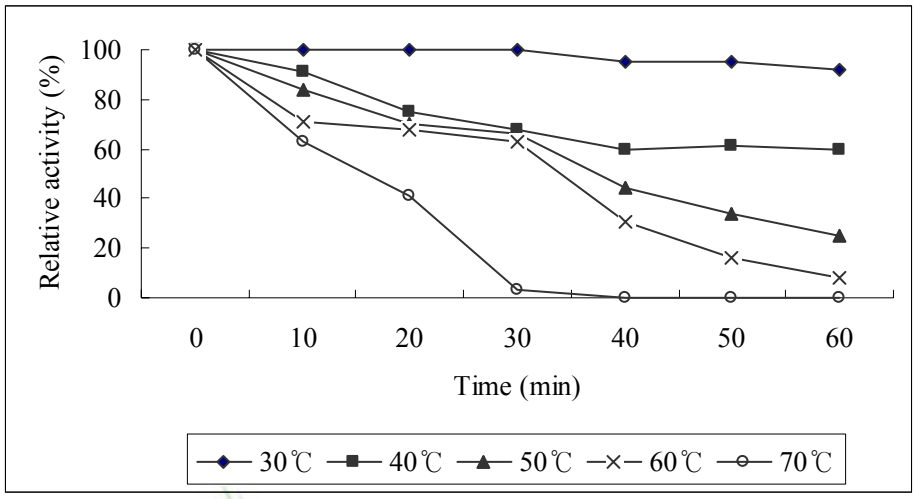

Fig. 12: Thermal stability of aCu,Zn-SOD. Enzyme activity at different temperatures was assessed by heating aliquots of enzyme at 30, 40, 50, 60 and 70 ^{o}C for 0, 10, 20, 30, 40, 50 and 60 min. The residual enzyme activity was determined

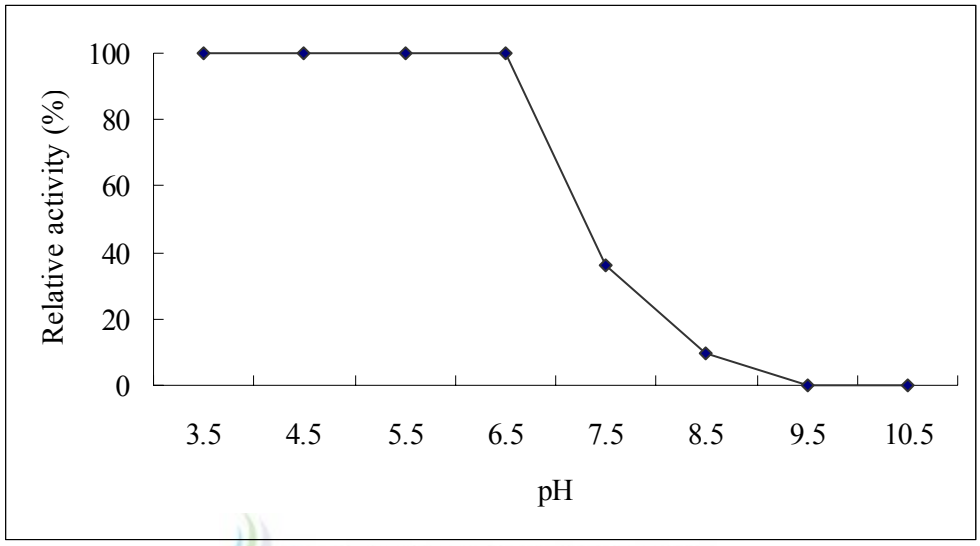

Fig. 13: Optimal pH of aCu,Zn-SOD. The enzyme activity was carried out in buffers with different pH values and relative activity was determined by xanthine oxidase method.

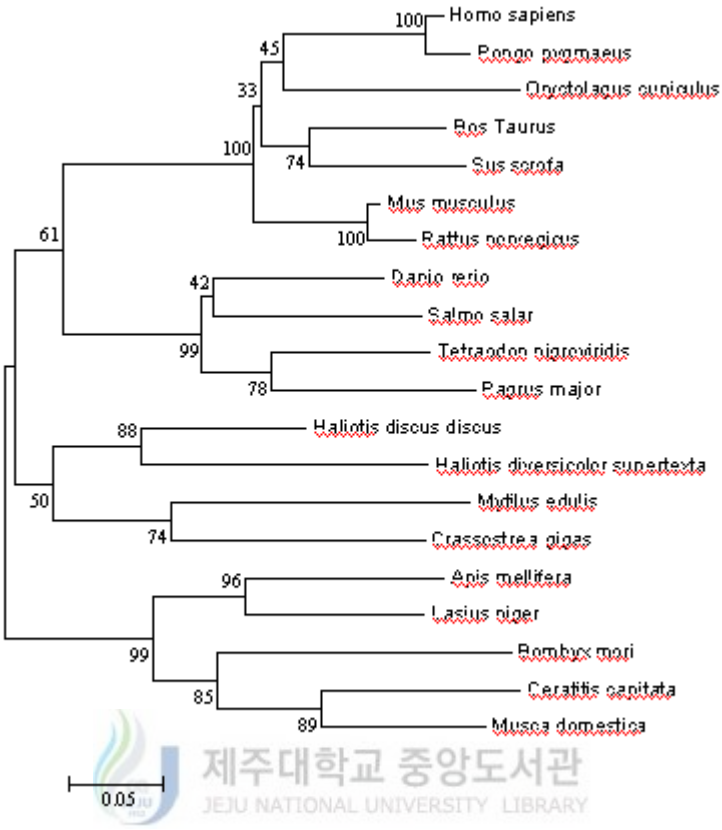

Fig. 14: A phylogenetic tree of CuZn-SOD proteins constructed by the Neighbor-Joining method with the PAM matrix model (MEGA 3.1, Kumar et al., 2004). Numbers at the nodes are Bootstrap values representing their robustness (1000 replications). Twenty species considered in the tree construction were *Homo sapiens*(NP000445),

Pongo pygmaeus (Q8HXQ4), *Oryctolagus cuniculus*(CAA80357), *Bos Taurus* (NP777040), *Sus scrofa* (PO4178), *Mus musculus* (NPO3564), *Rattus norvegicus*(NP058746), *Danio rerio*(NP571369), *Salmo salar* (AAW59361), *Tetraodon nigroviridis*(CAG00454), *Pagrus major*(AA015363), *Haliotis diversicolor supertexta*(AAY18806), *Mytilus edulis*(CAE46443), *Crassostrea gigas* (CAD42722), *Apis mellifera*(AAP93581), *Lasius niger*(AAQ81639), *Bombyx mori* (AAR97568), *Ceratitis capitata*(P28755) and *Musca domestica*(AAR23787).

4. DISCUSSION

Isolation of full length cDNA encoding Cu,Zn-SOD from *H. discus discus*:

By cloning and sequencing the putative aCu,Zn-SOD, a coding region of 465 bp nucleotides coding for a polypeptide of 154 amino acids, with an 74 bp 5' untranslated region and an 487 bp 3' untranslated region was identified (Fig. 8) with a predicted molecular weight of 16 kDa and a theoretical pI of 5.5. The length of the coding region is similar to most of the other Cu,Zn-SOD coding regions reported so far (Castellanos-Gonzalez et al., 2002). The major constituent of the protein was glycine accounting for 16% (Expert Protein Analysis System, proteomics server from the Swiss Institutes of Bioinformatics), which is common for aCu,Zn-SODs (Buettner, 1998). Comparison of aCu,Zn-SOD with other 47 known Cu,Zn-SOD sequences in the public database revealed 48 amino acid residues conserved in all Cu,Zn-SODs accounting to 29% homology at amino acid level.

Overexpression of a Cu,Zn-SOD in *E. coli* K12(TB1):

When aCu,Zn SOD was expressed in *E. coli* K12(TB1) and analysed using 12% Sodium-dodecyl sulfate polyacrylamide gel electrophoresis (SDS-PAGE), a distinct band with a high intensity emerged in IPTG induced sample (Fig. 9). The purified recombinant enzyme was obtained following the pMAL protein purification system, which made the purification profile simple and efficient. The homogeneity of the purified product was examined

by SDS-PAGE. The result derived by subtracting the value obtained from this analysis from that of corresponding to the fusion protein (42.5 kDa) coincided with the expected molecular weight of 16 kDa. The enzymatic activity of purified enzymes was 2461 Unit/mg when tested by the xanthine oxidase method described by Nagai et al. (1985). This value is moderate when compared with that of other recombinant Cu,Zn-SODs expressed. Activity observedin aCu,Zn-SOD is higher to the activity of zebrafish Cu,Zn-SOD expressed in AD494(DE3)pLysS (Ken et al., 2003) but lower to that of reported value for papaya Cu,Zn-SODs (Lin et al., 1998). When comparing the amino acid sequence between papaya with both zebrafish Cu,Zn-SOD and aCu,Zn-SOD, it was observed that Cys residue at position 7 in *H. discus discus* is replaced with Ala in plant. Hallewell et al. (1991) reported that buried Cys would interfere with the protein folding by forming an incorrect disulfide bond. Ken et al. (2003) suggests that further studies should be carried out using site-directed mutagenesis to replace Cys-7 to Ala-7 to observe the change of activity. In the recent history of expressing recombinant Cu,Zn-SODs, some studies have carried out enriching the growth media with external Cu and Zn sources to enhance the activity (Liu et al., 2002). According to the general accepted theory, the negative charge elsewhere on the protein surface reinforces the attraction by the positive channel around the copper. The enzyme-catalyzed dismutation by Cu,Zn-SOD is believed to proceed by subsequent reduction and oxidation of Cu ion acting as an electron carrier. The Zn atom is completely buried within the

protein structure and is suggested to play a structural role helping the protein stability (Ozturk-Urek and Tarhan, 2001).

Deduced Amino acid sequence comparison:

The deduced amino acid sequence from the cDNA of *H. discus discus* was compared with those of the *H. diversicolor supertext* (AAY18806)*, S. scrofa* (P04178), *G. gallus* (NP990395), *B. taurus,* (P00442) and *H. sapiens* (P00441) using the Clustal W program (Fig. 10). The alignment reveals that the *H. discus dicus* shares 78, 67, 66, 71 and 68% homology with *H. diversicolor supertext, S. scrofa*, *G. gallus*, *B. taurus,* and *H. sapiens* respectively. The close evolutional relationship between two abalone species was demonstrated by the highest homology between the two sequences. Altogether 82 amino acid residues were conserved among all 6 amino acid sequences accounting to 53% homology at amino acid level. Further, comparison of aCu,Zn SOD with three aquatic molluscs; *Ruditapes decussates, Dreissena polymorpha* and *Bathymodiolus azoricus* and mammalian Cu,Zn SODs (Geret et al., 2004) showed several residues maintaining the active site geometry being conserved (Gly45, Gly62, Pro75 and Gly83). The metal binding sites His47, -49, 64, -121 for copper and His64, 72, 81 and Asp84 for Zinc were also conserved in aCu,Zn-SOD. Two Cys residues which is believed to contribute towards forming the intra-chain disulfide bridge in mammalian Cu,Zn-SOD were found at Cys58 and Cys147. Three- dimensional structure predicted for aCu,Zn-SOD by Deep view –

spdbv 3.7, confirmed the potential of this disulfied bond formation between Cys58 and Cys147 (data not shown).

Optimal temperature and Thermal stability:

Temperature is a crucial factor that influences the rate at which an enzyme works. Thus, it is important to determine an optimal temperature for an enzymatic action. As shown in Fig. 11, aCu,Zn-SOD has its optimal activity at 37 ^{o}C. When exposed to temperatures varying from 25, 30, 37, 40, 50, 60, 70 and 80 ^{o}C, the enzymatic activity gradually decreased from 37 to 60 ^{o}C and then showed irreversible heat inactivation at 70 ^{o}C. Buettner (1998) has reported that Cu,Zn-SOD is disassociated by SDS and β-mercaptoethanol or EDTA and heat at 40-55 ^{o}C . Temperature to break apart 50% of Cu,Zn-SOD activity in 10 min is reported as 67 ^{o}C. It is also reported that Cu,Zn-SOD is stable to repeated freeze thaw cycles and prolonged refrigeration (4 ^{o}C) (Buettner,1998).

The thermal stability of aCu,Zn-SOD was detected with irreversible thermal denaturation at 70 ^{o}C after 20 minutes. During continuous incubation at varying temperatures from 30 to 70 ^{o}C, the residual enzymatic activity was assayed by means of the xanthine oxidase method. The result is plotted in Fig. 12. Similar observations were reported by Liu et al. (2002) for recombinant duck Cu,Zn-SOD where it had lower thermal stability compared to the control bovine Cu,Zn-SOD used in the experiment. Site directed mutagenesis studies indicated that free cystein residues might be the major molecular determinants for different protein stabilities among various Cu,Zn-

SODs (Hallewell et al., 1991). This suggestion is further confirmed by the studies reported of mutant human SOD Cys111Ser displaying higher thermal stability compared to those without mutation (McRee et al., 1990). Further, Bonaccorsi et al., (2000) have reported that Cys150 in *Xenopus laevis* SOD, which is quite sensitive to its heat resistance. In this manner, Cys147 in aCu,Zn-SOD, corresponding to Cys150 in *X. laevis* SOD, is very likely related to its thermal stability.

Optimal pH:

As shown in Fig. 13, aCu,Zn-SOD was very stable in an acidic pH range from pH 3.5 to 6.5. These results are consistent with the studies conducted by Ken et al., (2003), in which, recombinant zebrafish Cu,Zn-SOD has exhibited a broad range of pH stability from 2.3 to 12. However, in our study, we observed a sharp decline of activity after pH 6.5. Cu,Zn-SOD characterized from chicken liver was reported to have a similar pattern of activity with regard to pH. The activity of Cu,Zn-SODs is dependent on ionic strength and alkaline pH in a way that typically reflects the functional role of charged amino acid residues, in particular lysine (Rigo et al., 1975). At neutral pH however, the radical exists mainly as O_2^-, and the dismutation reaction is relatively slow due to electrostatic repulsion of the negatively charged radicals (Argese et al., 1984).

Phylogenetic analysis:

The phylogenetic tree of Cu,Zn-SOD protein sequences of *H. discus discus* and 19 other species shows close evolutionary relationship between

aCu,Zn-SOD and that of H. diversicolor supertexta (Fig. 7). Such relationship was strongly supported by a high bootstrap value (88%). Close relationships among the molluscs species were also supported (50%). The deuterostome vertebrates and the protostome invertebrates were grouped into distinct clades in the tree, representing that the evolution of CuZn-SODs reflects the evolutionary history of the animal phyla (Fig. 7).

The structural core of Cu,Zn-SOD exists as a Greek key β-barrel motif, consisting of eight β-barrels (Getzoff et al., 1989). The amino acid substitution, as well as deletions and insertions, occurs mostly outside of this structural motif. It is reported that Cu,Zn-SOD has experienced a significant changes in its evolutionary rate (Smith and Doolittle, 1992). Both prokaryotic and eukaryotic Cu,Zn-SOD have similar metal binding residues in the same sequence and structural order, indicating the active site of of Cu,Zn-SOD predates the emergence of eyokaryotes (Forest et al., 2000).

In conclusion, gene encoding the abalone (*H. discus discus*) Cu,Zn-SOD was sequenced, and the recombinant Cu,Zn-SOD was successfully overexpressed in *E. coli* K12(TB1) cells and characterized. This information on the *H. discus discus* Cu,Zn-SOD sequence may provide a framework for future studies on the role of Cu,Zn-SOD in marine invertebrates.

Part III

Cloning, expression, purification and characterization of Mn-superoxide dismutase from abalone (*Haliotis discus discus*) cDNA

1. ABSTRACT

The mitochondrial enzyme manganese-superoxide dismutase (Mn-SOD) is one of the primary proteins involved in cellular defense against oxidative stress and catalyzes the conversion of superoxide into the stabler hydrogen peroxide. In this study, a putative gene encoding Mn-SOD from disk abalone (*Haliotis discus* discus) (aMn-SOD) cDNA library was sequenced, cloned, expressed in *E. coli* K12(TB1) and the protein was purified using pMAL protein purification system. Sequencing resulted 930 bp region with a protein encoding region of 682 bp, which corresponded to 226 amino acids. The pI value of the expected protein was 6.5. The protein was expressed in soluble form with molecular weight of 25 kDa + 42.5 kDa maltose binding protein. The fusion protein had 2781 U/mg activity when assayed by xanthene oxidase method. The optimum temperature of the enzyme was 37 ^{o}C and it was active in a range of acidic pH (from 3.5 to 6.5). The enzyme activity was reduced to 50% at 50 ^{o}C and completely heat inactivated at 80 ^{o}C. The alignment of aMn-SOD amino acid sequence with 35 known Mn-SODs by CLSTAL W program revealed that conservation of 68 amino acid residues and 30% homology. In comparison with human Mn-

SOD, all manganese-binding sites are also conserved in aMn-SOD (H_{28}, H_{100}, D_{185} and H_{189}). Understandingly, the aMn-SOD amino acid sequence was closer to that of *Biomphalaria glabrata* than to others in phylogenetic analysis.

2. MATERIALS AND METHODS

Sequencing of the gene encoding aMn-SOD:

A clone with expected function of Mn-SOD was selected from abalone cDNA library. The plasmid DNA of the putative aMn-SOD was isolated by the Accuprep^{TM} plasmid extraction kit (Bioneer Co., Korea). The full-length sequence was determined by sequencing with oligo dT primer. After deriving the full length, the sequence was compared against the National Center for Biotechnology Information (NCBI) databases by BLAST-X

Cloning the coding sequence of aMn-SOD into pMAL expression vector:

Having checked the restriction enzyme sites of the aMn-SOD sequence, a pair of primers was designed for cloning the coding sequence of the aMn-SOD into expression vector, pMAL-c2X (New England Biolabs, USA). The sense amplification primer was designed as 5'-gagaggaGAATTCATGTTGTCTGCTACGCTCTCT -3' having a *Eco*R I site and an antisense primer 5'- gagagaCTGCAGGGCCGCAAGTTTGGCTT-3' containing *Pst* I site. In a total of 50 µl of PCR reaction, 5 units of Ex Taq polymerase (Takara Korea Biomedical Inc., Korea), 5 µl of 10X Ex Taq buffer, 4 µl of 2.5 mM dNTP, 50 ng of template, 50 pmol of each primer were used. After initial incubation at 94 ^{o}C for 2 min, 25 cycles were carried out with 30 sec denaturation at 94 ^{o}C, 30 sec of annealing at 55 ^{o}C, and 40 sec of elongation at 72 ^{o}C, followed by a final extension at 72 ^{o}C for 5 min. The PCR product was analysed using 1% agarose gel and ethidium bromide

staining. Thereafter it was purified by the Accuprep^{TM} gel purification kit (Bioneer Co., Korea) and digested with *EcoR* I and *Pst* I restriction enzymes. The expression vector, pMAL-c2X, was digested with the same restriction enzymes as the PCR product and dephosphorylated with calf intestine phosphatase (NEB, USA) according to the vendor's protocol. Thereafter the vector and PCR product was purified by a 1% agarose gel using Qiaex-II gel purification Kit (QIAGEN Inc., USA).

Ligation was carried out at 16 ^{o}C, overnight with 100 ng of pMAL-c2X vector, 25 ng of PCR product, 1 µl of 10X ligation buffer and 0.5 µl 1X T4DNA ligase (Takara Korea Biochemical Inc., Korea). The ligated product was transformed into XL1 cells. The correct recombinant confirmed by colony cracking, restriction enzyme digestion, and sequencing was transformed into the competent cells; *E. coli* K12 (TB1).

Overxpression of aMn-SOD:

The recombinant enzyme was overexpressed in *E. coli* K12(TB1) cells in the presence of 0.5 mM isopropyl-ß-thiogalactopyranoside (IPTG). A volume containing 10 ml of starter culture was inoculated into 100 ml Luria broth with 100 µl ampicillin (100 mg/ml) and 10 mM glucose (2% final concentration) and kept at 37 ^{o}C with 200 rpm until OD_{600} approached 0.5. The culture was then shifted to 20 ^{o}C for 15 min prior to induction with 1 mM IPTG at the final concentration. After 3 hrs of induction, the cells were cooled on ice for 30 min and harvested by centrifugation at 4000 rpm for 20 min at 4 ^{o}C. The cells were re-suspended with 5 ml column buffer (Tri-HCl,

pH 7.4, 200mM NaCl) and frozen in liquid nitrogen and stored in -70 ^{o}C freezer.

Purification of aMn-SOD:

The pMAL^{TM} protein fusion and purification system was followed. In brief, amylose resin was poured into a 1 x 5 cm column and washed with 8 x column volumes of column buffer. The diluted crude extract was loaded at a flow rate of 1 ml/hr. The column was then washed with 12 x column volumes of column buffer and the fusion protein was eluted with elution buffer (column buffer + 10 mM maltose). The elute was collected in 500 μl fractions. The eluted protein content was measured by UV absorbance at 280 nm. SDS-PAGE was performed according to the standard procedure for discontinuous SDS-PAGE. The stacking and separating gels were prepared at 12% and 5% respectively and the gel was stained with Coomassie blue.

Mn-SOD activity assay and determination of protein concentration:

Activity of aMn-SOD was detrmined by the xanthine oxidase method according to the procedures described by Nagai et al (2003). The reaction mixture consisted of 0.48 ml of 0.05 M sodium carbonate buffer (pH 7.5), 0.02 ml of 3 mM xanthine, 0.02 ml of 3 mM EDTA, 0.02 ml of 0.15% bovine serum albumin, 0.02 ml of 0.75 mM NBT and 0.02 ml of enzyme sample. After incubation at 25 °C for 10 minutes, the reaction was initiated by adding 6 mU xanthine oxidase and maintaining the temperature at 25 °C for 20 min. The reaction was stopped by adding 0.02 ml of 6 mM CuCl. The absorbance was recorded in a microplate reader (Sunrise; Tecan Co. Ltd.,

Austria) at 560 nm. Fifty percent inhibition of the reaction was considered as one enzyme unit. The protein concentration was determined by the procedure of Lowrey et al. (1951) using bovine serum albumin as the standard.

In order to determine the optimal temperature, each reaction was carried out at 25, 30, 37, 40, 50, 60, 70 and 80 ^{o}C and the relative activity was determined. To determine the optimal pH of the aMn-SOD each reaction was carried out in acetate buffer pH 3.5, acetate buffer pH 4.5, acetate buffer pH 5.5, phosphate buffer pH 6.5, phosphate buffer pH 7.5, glycine-NaOH buffer pH 8.5, glycine-NaOH buffer pH 9.5 and glycine-NaOH buffer pH 10.5 and the relative activity was determined.

Analysis of nucleotide and amino acid sequences:

Nucleotide sequence analysis was performed with the DNAssit program (version 2.2). The NCBI BLAST program (http://www.ncbi.nlm.nih.gov) was used to search for nucleotide and protein sequences similar to the abalone Mn-SOD. Protein sequence analysis was performed with the CLUSTAL W Multiple Sequence Alignment Program (version 1.8, 1999). Phylogenetic relationship was determined by MEGA 3.0 program (Kumar et al., 2004). The phylogenetic tree was constructed using the Neighbour-joining method.

3. RESULTS

```
                                                GGGGAAAGTATTCGTCGTTTGTGCTGAACCAGGCCTCAAAC   41

ATGTTGTCTGCTACGCTCTCTGCTGTAAAAAGGGCAGTGCCTTCTCCAGCATGGCTTGCTACAGCAGCCGTGAGGATGAAGCAC  125

M--L--S--A--T--L--S--A--V--K--R--A--V--P--S--P--A--W--L--A--T--A--A--V--R--M--K--H--

ACACTGCCAGACCTCCCCTACGACTATAATGCTCTCGAGCCCTACATCTCGGCTGACATCATGAAGCTTCACCACAAGAAGCAT  209

T--L--P- D--L--P--Y--D--Y--N--A--L--E--P--Y--I--S--A-D--I--M--K--L--H--H--K--K--H--H

CACAACGCCTACGTCACAAACCTCAATGTGGCTCAGGAGAAACTGTCTGAAGCAGAGGCAAAAAACGATATTAACAGCATCATT  293

--N--A--Y--V--T--N--L--N--V--A--Q--E--K--L--S--E--A--E--A--K--N--D--I--N-- S--I--I--

TCACTCCAGCCATCCCTCAGGTTCAATGGCGGAGGACATATCAACCACTCCATCTTCTGGGAGGTGCTTAGCCCAAATGGTGGC  377

S--L--Q--P--S--L--R--F--N--G--G--G--H--I--N--H--S--I--F--W--E--V--L--S--P--N--G-G--G

GGGGAACCGGATGGGGACCTCATGCACTGCATCAAACGTGACTTTGGTTCATACGATGAAATGAAGAAAGAGCTTACTGCTTCA  461

--E--P--D--G--D--L--M--H--C--I--K--R--D--F--G--S--Y--D--E--M--K--K--E--L--T--A--S--A

GCTGTGACAGTCCAGGGCTCAGGGTGGGCGTGGCTTGGGTTTAACCCGGTCAGTGGCCGTTTGAGAGTGTCTGCCTGTGCTAAC  545

--V--T--V--Q--G--S--G--W--A--W--L--G--F--N-P-V--S--G--R--L--R--V--S--A--C--A--N--Q--

CAAGATCCCCTGGAGGCTACAACAGGACTGGTTCCCCTCTTTGGCATCGATGTCTGGGAACACGCATACTATCTCCAATACAAG  629

D--P --L--E--A--T--T--G--L--V--P--L--F--G--I--D--V--W--E--H--A--Y--Y--L--Q--Y--K--N

AATGTGAGGCCAGATTATGTTGGTGCTATTTTCAGTGTTGCCAACTGGGAAAATGTGGCCCGAAGACTATCAGAAGCCAAACTT  713

--V--R--P--D--Y--V--G--A--I--F--S--V--A--N--W--E--N--V--A--R--R--L-- S--E--A--K--L--

GCGGCCtgaGAAGTTCATGACTCACGACAAAAACAGTGAACTGTGTATAAAATGAGACTTACTTACCCAAGGAAAGATCTGTAC  797

A--A--

CTGATGCTGGGTGTGGAATGATGAAAATTGCATTTGACATTAGTAGACATTGAAATATGTTACAAATATGATGATTTAATCATG 991
```

ACTGAAAGATTTTTGATCTGGCTTTAAAACACGTACTGCTAATCATTCGG 931

Fig. 15: Nucleotide sequence and the deduced amino acid sequence of aMn-SOD. The coding sequence (from 42 to 690) is in bold letters. Amino acid sequence corresponding to the protein consists of 226 amino acids. The neucleotide from 1 to 41 and 719 to 931 indicate 5' UTR and 3' UTR respectively. Putative signal peptide is underlined. The residues related to coordination of Mn ion are shaded. Putative Mn-SOD signature is boxed.

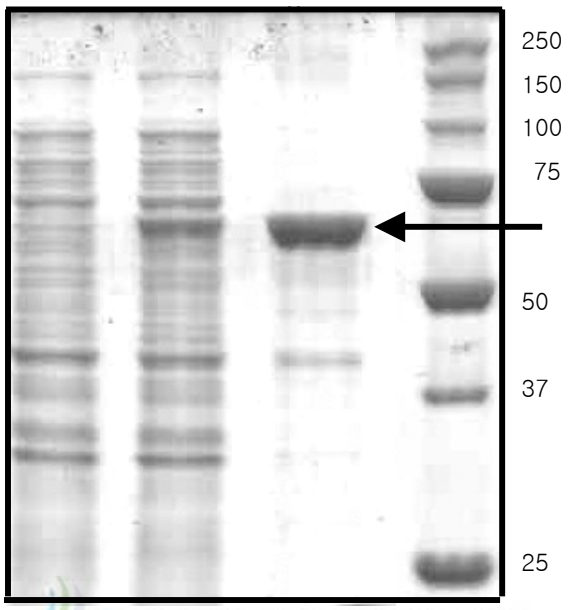

Fig. 16: Analysis of aMn-SOD protein expressed in *E. coli* K12 (TB1) cells following purification in a 12% denaturing polyacrylamide gel. A: before induction with IPTG; B: after cells were induced with 0.5 mM IPTG and grown at 20 ^{o}C for 3 hrs; C: Recombinant protein purified under native conditions by pMAL^{TM} Protein Fusion and purification system. D: Biorad precision plus protein standard

```
homo_sapiens                ----MLSRAVCGTSRQLAPALGYLGS-RQKHSLPDLPYDYGALEPHINAQ
Pongo_pygmaeus              ----MLSRGVCGTSRQLAPALGYLGS-RQKHSLPDLPYDYGALEPHINAQ
Bos_taurus                  ----MLSRAACSTSRRLVPALSVLGS-RQKHSLPDLPYDYGALEPHINAQ
Rattus_norvegicus           ----MLCRAACSAGRRLGPAASTAGS-RHKHSLPDLPYDYGALEPHINAQ
Melopsittacus_undulatus     --MLCRLSSAGRSSVKVVAPLGCLAS-RQKHTLPDLPYDYGALQPHISAE
Gallus_gallus               --MLCRLASAGRSRAALVAPWGCLVA-RQKHTLPDLPYDYGALEPHISAE
Epinephelus_coioides        --MLCRVGQIRRCAASLNQTINQVAASRQKHTLPDLTYDYGALEPHINAE
Danio_rerio                 --MLCRVGYVRRCAATFNPLLGAVTS-RQKHALPDLTYDYGALEPHICAE
H._discus                   ---MLSATLSAVKRAVPSPAWLATAAVRMKHTLPDLPYDYNALEPYISAD
Biomphalaria_glabrata       MSKMLSTTSSSLKRCFG------VSLLRLKHTLPDLKYDFNALEPYISAD
                                                     * **:**** **:.**:*:* *:

homo_sapiens                IMQLHHSKHHAAYVNNLNVTEEKYQEALAKGDVTAQIALQPALKFNGGGH
Pongo_pygmaeus              IMQLHHSKHHAAYVNNLNVTEEKYQEALAKGDVTAQIALQPALKFNGGGH
Bos_taurus                  IMQLHHSKHHAAYVNNLNVAEEKYREALEKGDVTAQIALQPALKFNGGGH
Rattus_norvegicus           IMQLHHSKHHATYVNNLNVTEEKYHEALAKGDVTTQVALQPALKFNGGGH
Melopsittacus_undulatus     IMQLHHSKHHATYVNNLNVAEEKYKEALAKGDVTAQVSLQPALKFNGGGH
Gallus_gallus               IMQLHHSKHHATYVNNLNVTEEKYKEALAKGDVTAQVSLQPALKFNGGGH
Epinephelus_coioides        IMQLHHSKHHATYVNNLNVTEEKYQEALAKGDVTTQVALQPALKFNGGGH
Danio_rerio                 IMQLHHSKHHATYVNNLNVTEEKYQEALAKGDVTTQVSLQPALKFNGGGH
H._discus                   IMKLHHKKHHNAYVTNLNVAQEKLSEAEAKNDINSIISLQPSLRFNGGGH
Biomphalaria_glabrata       IMKLHYQKHHQAYVNNLNVAEEKLKAAVDKGDVNTIISLQPALKFNGGGH
                            **:**:.*** :**.****::**   *  *.*:.: ::***:*:******

homo_sapiens                INHSIFWTNLSPNGGGEPKGELLEAIKRDFGSFDKFKEKLTAASVGVQGS
Pongo_pygmaeus              INHSIFWTNLSPNGGGEPKGELLEAIKRDFGSFDKFKEKLTAASVGVQGS
Bos_taurus                  INHSIFWTNLSPNGGGEPQGELLEAIKRDFGSFAKFKEKLTAVSVGVQGS
Rattus_norvegicus           INHSIFWTNLSPKGGGEPKGELLEAIKRDFGSFEKFKEKLTAVSVGVQGS
Melopsittacus_undulatus     INHTIFWTNLSPNGGGEPKGELMDAIKRDFGSFANFKEKLTAVSVGVQGS
Gallus_gallus               INHTIFWTNLSPSGGGEPKGELMEAIKRDFGSFANFKEKLTAVSVGVQGS
Epinephelus_coioides        INHTIFWTSLSPNGGGEPQGELMEAIKRDFGSFQKMKEKMSAATVAVQGS
Danio_rerio                 INHTIFWTNLSPNGGGEPQGELLEAIKRDFGSFQKMKEKISAATVAVQGS
H._discus                   INHSIFWEVLSPNGGGEPDGDLMHCIKRDFGSYDEMKKELTASAVTVQGS
Biomphalaria_glabrata       INHTIFWSNLSPKGGGEPTGDLLQLIKEEFSTFENMKKLLAEKSVAIQGS
                            ***:***  ***.***** *:*:. **.:*.:: ::*: ::  :* :***
```

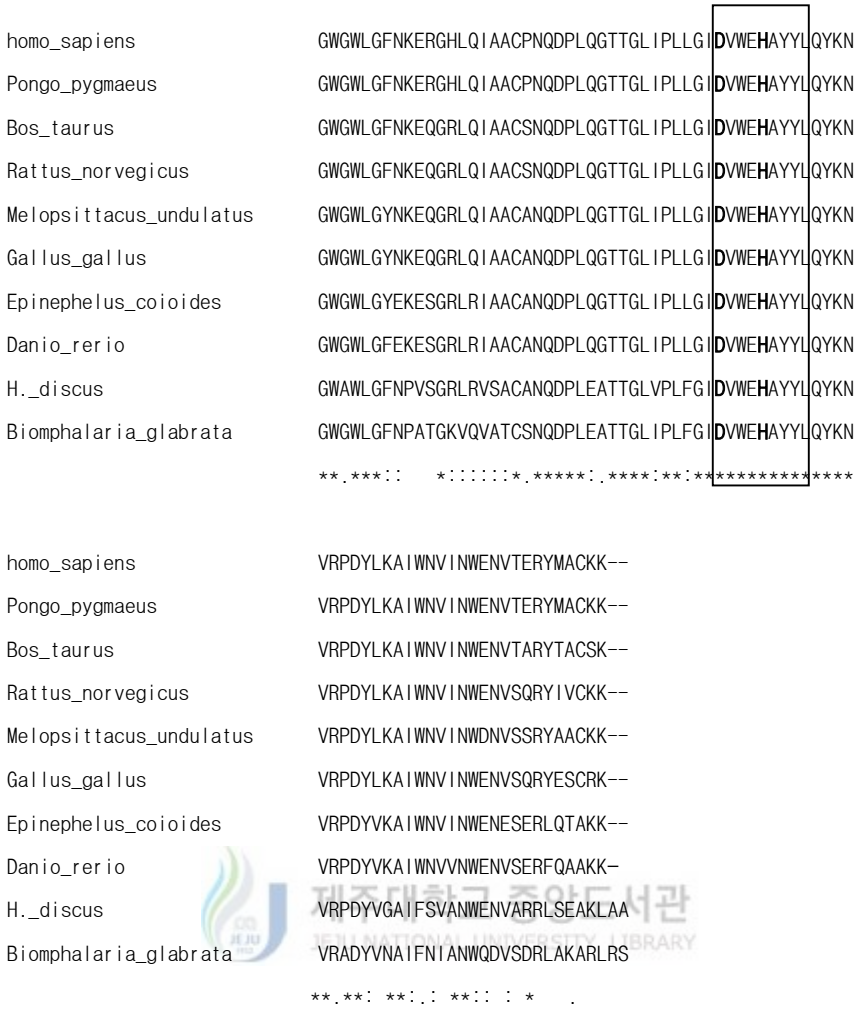

Fig. 17: Multiple sequence alignments of aMn-SOD with 9 other (human erythrocyte- CAA42066, *P. pimaeus*- CAH93471, *B. Taurus*-151918, *R. norvegicus*-NP08747, *M. undulates*-AAO72712, *G. gallus*- NP989542, *E. coioides*-AAW29024, *D. rerio*- NP956270 and *B. glabrata*- AA583981) known Mn-SOD amino acid sequences. The alignment program Clustal W automatically

introduces gaps (dash) to maximize similarity among the primary structures of these. All amino acid residues identical to corresponding ones of aMn-SOD are represented with asterisks. Conserved substitutions depending on functionality are indicated with colon and the semi-conserved residues with a dot. Putative Mn-SOD signature is boxed. The residues related to coordination of Mn ion conserved in all 9 species are shaded.

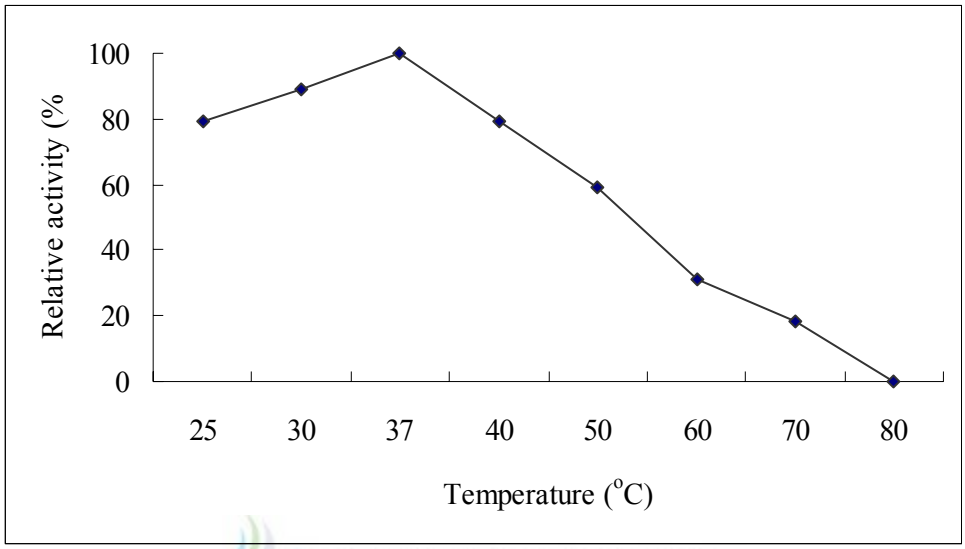

Fig. 18: Optimal temperature of aMn-SOD. Enzyme activity was carried out at different temperatures (25, 30, 37, 40, 50, 60, 70 and 80 ^{o}C) and relative activity was determined by xanthine oxidase method.

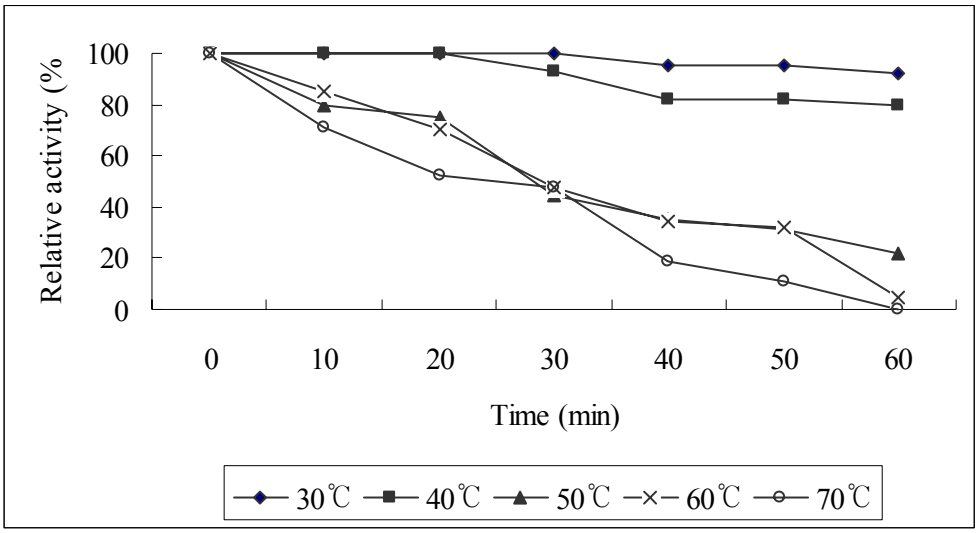

Fig. 19: Thermal stability of aMn-SOD. Enzyme activity at different temperatures was assessed by heating aliquots of enzyme at 30, 40, 50, 60 and 70 ^{o}C for 0, 10, 20, 30, 40, 50 and 60 min. The residual enzyme activity was determined

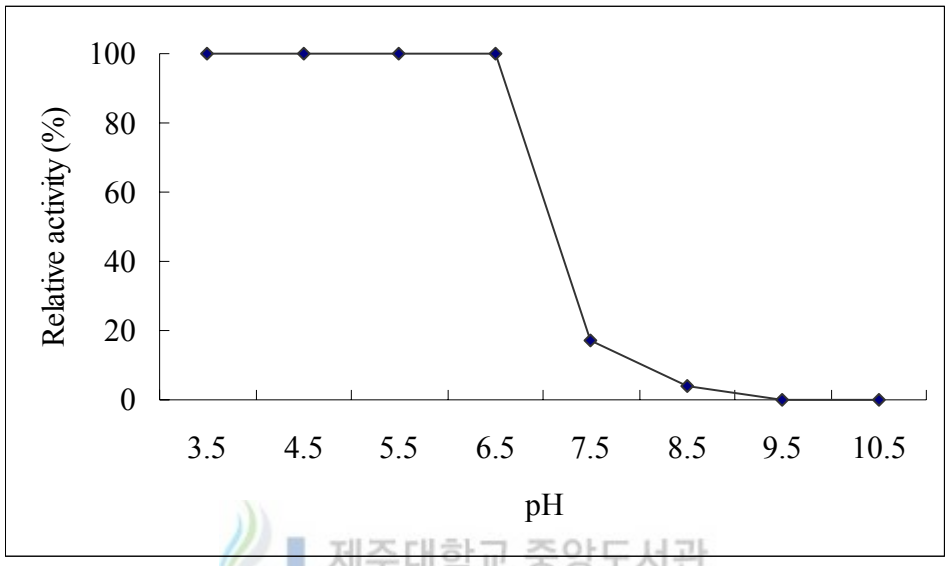

Fig. 20: Optimal pH of aMn-SOD. The enzyme activity was carried out in buffers with different pH values and relative activity was determined by xanthine oxidase method.

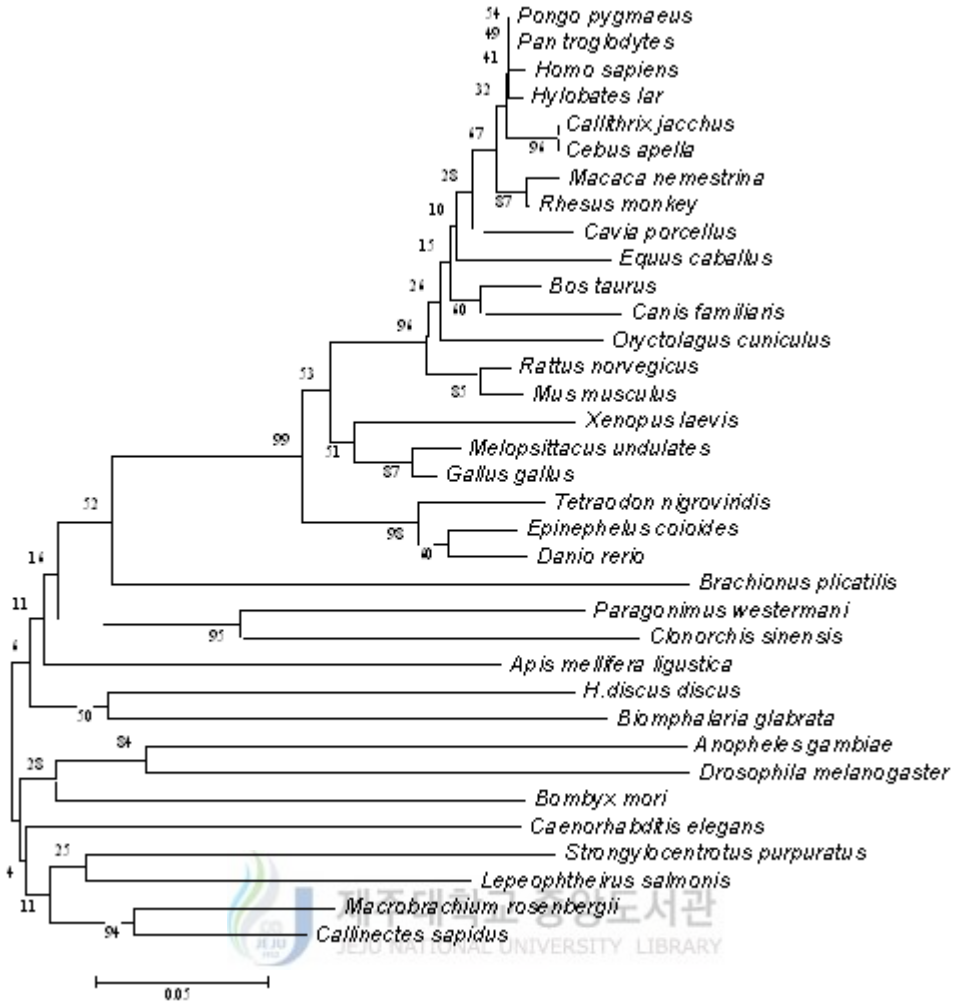

Fig. 21: Neighbor-joining tree based on Mn-SOD amino acid sequences obtained from 35 species. (MEGA 3.0, Kumar et al., 2004). Bootstrap values (1000 replications) are displayed over internal nodes.

4. DISCUSSION

Cloning and analyzing abalone Mn-SOD:

In invertebrates, the enzymes involved in acting on ROS are NADPH-oxidase, SOD, peroxidase, catalase and glutathione peroxidases. SOD catalyses the rapid two step dismutation of the toxic superoxide anion into molecular oxygen and hydrogen peroxide through the alternate reduction and oxidation of the active-metal ion (Smith and Doolittle, 1992). Fig. 15 presents the nucleotide and deduced amino acid sequence of putative aMn-SOD gene. Sequecne analysis resulted an open reading frame of 690 bp coding for 226 amino acid residues. The neucleotide sequence from 1 to 41 and 731 to 929 indicate an 5' UTR and an 3' UTR respectively. Putative signal peptide region of 22 amino acids was identified within the aMn-SOD coding sequence by SignalP V3.0 World Wide Web Server (Bendtsen et al. 2004). Signal peptide of 23 amino acids for primate Mn-SOD has also been reported (Fukuhara et al., 2002). The function of this presumed signal peptide is reported as translocation of Mn-SOD into mitochondria. In eukaryotic cells, Mn-SOD is synthesized in the cytosol and then imported post-traslationally into the mitochondrial matrix. (Bannister et al., 1987; Keele et al., 1970). The main four residues (H28, H100, D185, and H189), which are putatively required for the co-ordination of the single trivalent manganese are conserved in aMn-SOD as they are reported in other Mn-SODs (Jackson and Cooper, 1998). In addition, 9 out of 11 residues that involve in putative active center of *Tatumella ptyseos* (H28, Y35, H97, H100,

W104, Q145, D195, W197 and H199) (Ken et al., 2005) are also conserved in this sequence. According to Stallings et al., (1985), out of the above residues, H28 and Y35 are supposed to contribute to form the helical confirmation, which is crucial for Mn-SOD catalytic based on the structure of Mn-SOD from *Thermus thermophilus* at 2.4-A^{o} resolution. Further, Mn-SOD signature shown in decapod crustaceans (DVWEHAYY) (Cheng et al., 2006) is also conserved in aMn-SOD (from amino acid 184 to 191).

The alignment of aMn-SOD amino acid sequence with 35 known Mn-SODs in NCBI database using CLUSTAL W program revealed a conservation of 68 amino acid residues and 30% homology. Fig. 17 shows the alignment of aMn-SOD with that of human erythrocyte- (CAA42066), *P. pimaeus* (CAH93471), *B. Taurus* (151918), *R. norvegicus* (NP08747), *M. undulates* (AAO72712), *G. gallus* (NP989542), *E. coioides* (AAW29024), *D. rerio* (NP956270) and *B. glabrata* (AA583981) showing 62, 62, 61, 60, 64, 62, 61, 61 and 62% homology respectively. Most of the regions required for activity are conserved in all compared Mn-SODs including four residues required for coordination of Mn ion and the Mn-SOD signature site (184-191 a.a).

Overexpression of aMn-SOD in *E. coli* K12(TB1):

aMn-SOD was successfully overexpressed in *E. coli* K12(TB1) when induced with 0.5 M IPTG (Fig. 16). Mn-SOD is produced in cytosol in the form of precursor, which is imported to mitochondrial matrix post-translationally. Precursor is supposed to be clipped by protease in inner

mitochondrial membrane until proteolytic processing takes place (Buettner, 1998). The expressed protein was easily purified with pMAL protein purification system. The purified protein had a molecular weight of 25 kDa after subtracting the molecular weight of maltose binding protein, which is 42.5 kDa. The theoretical isoelectric point of the protein was calculated to be 6.5. The highest constituent was alanine (11%). Most of the reported molecular weights for Mn-SOD range from 20-40 kDa (Babitha et al., 2002). The isoelectric points also vary from 4.0 - 6.5. The purified enzyme showed 2781 U/mg activity. This value is almost similar to the Mn-SOD activity reported from *Thermus aquaticus* (Motoshima et al., 1998) but lesser to the unusually stable Mn-SOD reported from *Tatumella ptyseos* ct (Ken et al., 2005).

Optimal temperature and thermal stability:

The enzyme had temperature optima at 37 ^{o}C (Fig. 18)**.** Until 70 ^{o}C, the activity retained up to 50% and then decreased. Above 80 ^{o}C, the enzyme was almost inactivated. Similarly, Wilde and Yu, (1998) have reported that increment in temperature up to 37 ^{o}C has increased Mn SOD activity in mung bean. Even though, Mn-SOD is reported to subject to freeze thaw inactivation (Buettner, 1998), Ken et al. (2005) have reported an unusual thermo-stable Mn-SOD from *Tatumella ptyseos* ct, having thermal inactivation rate constant κ_d as 0.015 min^{-1} at 80 ^{o}C. In contrast, Mn-SOD from pearl millet seedlings had showed less thermo stability (Babitha et al.,

2002). The aMn-SOD activity reduced by 50% when heated for 30 min at 50 ^{o}C (Fig .19).

Optimal pH:

The effect of pH on the purified enzyme is shown in Fig. 20. Optimum activity was obtained in the range of buffer from pH 3.5- 6.5. The enzyme retained 100% activity during this range and then drastically decreased to 20% at pH 7.5. The enzyme was totally inactivated at pH 9.5 and above. In contrast, the optimum pH for SOD activity in mung bean and corn was reported to be 7.8 (Wilde and Yu, 1998; Giannopolitis and Rios, 1977). However, studies conducted by Ken et al., (2005) shows that acidic pH is favorable to form monomer of the protein than the non-acidic pH. This could be a probable reason of aMn-SOD demonstrating high activity in acidic pH. Buettner (1998) has also reported that Mn-SOD is an acidic protein with decreasing activity with increasing pH, specially with pH greater than 7.8. This characteristic of aMn-SOD could broaden its application in industry.

Phylogenetic analysis:

The appearance of SOD enzymes was triggered by the proliferation of photosynthetic organisms that began to produce oxygen about 2 billion years ago. Zelko et al. (2002) reports that the evolutionary rates of Mn-SOD has been constant compared to Cu,Zn-SOD during the last billion years. We aligned the amino acid sequence of aMn-SOD with 35 other Mn-SODs using Clustal W program. Phylogenetic analysis on the aligned sequences was

performed using the method of neighbour-joining (Fig. 21). According to the findings, aMn-SOD is closer to that of *Biomphalaria labrata* (fresh water snail) than to others in the phylogenetic tree. This confirms the close evolutionary linkage between two molluscs. Fukuhara et al. (2002) suggests that Mn-SOD could be a suitable candidate to use as a molecular marker for evolutionary studies as Mn-SOD has shown to be a single copy in mammals. In this manner, this study on aMn SOD could also contribute to future studies in evolution of invertebrate Mn-SODs.

In conclusion, for the first time, the gene encoding Mn-SOD from abalone (*Haliotis discus* discus) was sequenced and the recombinant Mn-SOD expressed in *E.coli* cells was characterized. This information on the aMn-SOD may be useful in benchmarking studies of Mn-SOD sequence analysis in marine invertebrates.

SUMMARY

Antioxidant enzymes are given high priority in current research due to the vital role they play in balancing the oxido-redox potential in the body. In this study, genes encoding three important antioxidant enzymes namely, catalase (aCAT), Cu,Zn- superoxide dismutase (aCu,Zn-SOD) and Mn-superoxide dismutase (aMn-SOD) were sequenced, cloned and analysed from the disk abalone (*Haliotis discus discus)* cDNA library. Firstly, after deriving the full length, the sequences were compared with the respective sequences in the public data base and attempts were made to identify the conserved regions in the sequences when compared with that of other organisms in order to establish the structure and functional relationships. As the second step, primers were designed to amplify the coding sequences (CDS) and amplicants were cloned into pMAL-c2X vector. Successful clones were transformed into either *E. coli* BL21(DE3) or K12(TB1) and the respective proteins were expressed in the presence of IPTG. Optimal temperature, pH and thermal stability of the expressed proteins were determined. The phylogenetic tree of each enzyme was built by the neighbour-joining method.

Catalase, which catalyses the reaction of H_2O_2 into H_2O and O_2, is an important enzyme which detoxifies the cellular H_2O_2. The catalase found in abalone belonging to true catalase group, comprises 1,503 bp ORF coding for 501 amino acids. It had 30,000 U/mg activity and was thermo stable in a broad range of pH (5.0-10.5) and temperatures. The enzyme was heat

inactivated at 80 ^{o}C. When compared with 22 other known catalase amino acid sequences, 173 residues were conserved in the aCAT amino acid sequence accounting to 34.5% homology. Among the compared sequences, aCAT was similar to Pacific white shrimp.

Superoxide dismutase (SOD) is the only antioxidant enzyme that acts on a free radical (O_2^-). SODs can be grouped according to the location or the active metal ion involved in it. aCu,Zn-SOD has a CDS of 465 bp coding for a 154 amino acid sequence and a molecular weight of 16 kDa with a pI value of 5.5. The optimum temperature of aCu,Zn-SOD was 37 ^{o}C and it was heat inactivated at 70 ^{o}C. It was active in a range of acidic pH (3.5-6.5). A comparison of aCu,Zn-SOD with that of 47 other species revealed the conservation of 48 amino acids and 29% homology. All the residues for Cu and Zn ion binding were conserved in aCu,Zn-SOD. According to phylogenetic studies, aCu,Zn-SOD is closer to that of *H. diversicolor supertext*, which is another abalone specie confirming the close evolutionary relationship between the two species.

Mn-SOD is produced in cytosol but imported into mitochondria post-translationally. aMn-SOD consists of 690 bp coding for a pre-protein of 226 amino acid with a signal peptide of 25 amino acids. The molecular weight of the expressed aMn-SOD is 25 kDa and the optimal temperature is 37 ^{o}C. In consistant with aCu,Zn-SOD, aMn-SOD was also active in acidic pH. The enzyme showed irreversible thermal inactivation at 80 ^{o}C. The aMn-SOD amino acid sequence was closer to that of fresh water snail (*Biomphalaria*

labrata) when compared with 35 other Mn-SOD amino acid sequences in the public database.

This information on successfully sequenced, cloned, overexpressed, purified and characterized CAT, Cu,Zn-SOD and Mn-SOD from abalone (*Haliotis discus discus*) and their sequence analysis may contribute to the comparative genomic studies on invertebrate antioxidant enzymes and their evolution.

REFERENCES

Argese, E., A. Rigo, P. Viglino, E. Orsega, F. Marmocchi, D. Cocco, and G. Rotilo. (1984). A Study of the pH Dependence of the Activity of Porcine Cu,Zn Superoxide Dismutase, *Biochim Biophys Acta*. 787: 205-211.

Babitha, M.P., H.S. Prakash and H. Shekar-Shetty. (2002). Purification and partial characterization of manganese superoxide dismutase from downy mildew resistant pearl millet seedlings inoculated with *Sclerospora graminicola. Plant Sci.* 163: 917-924.

Bannister, J.V., W.H. Bannister and G. Rotilio. (1987). Aspects of the Structure, function, and applications of superoxide dismutase. CRC Crit. *Rev. Biochem*. 22: 111-180

Bendtsen, J. D., H. Nielsen, G. Von-Heijn and S. Brunak (2004). Improved prediction of signal peptides: SignalP 3.0. *J. Mol. Biol*. 340:783-795.

Benedetto, M.T., Y. Anzai and J.W. Gordon. (1991). Isolation and analysis of the mouse genomic sequence encoding Cu-Zn superoxide dismutase. *Gene.* 99: 191-195.

Bernard, D., B. Quatannens, A. Begue, B. Vandenbunder and C. Abbadie. (2001). Antiproliferative and Antiapoptotic Effects of cRel May Occur within the Same Cells via the Up-Regulation of Manganese Superoxide

Dismutase. *Cancer Res*. 61: 2656-2664.

Beyer, W., J. Imlay and I. Fridovich. (1991). Superoxide dismutases. *Prog. Nucleic Acid res*. *Mol. Biol.* 40: 221-253.

Birnboim, H.C. and M. Kanabus-Kaminka. (1985). The production of DNA strands breaks in human leukocytes by superoxide anion may involve a metabolic process. *Proc. Natl. Acad. Sci.* USA 82: 6820-4.

Bonaccorsi-de-Patti, M.C., M.T., Carri, R.Gabbianelli, R. Da-Gai, C.Volpe, A. Giartosio, G. Rotilio and A. Battistoni. (2000) A free cysteine residue at the dimmer interface decreases conformational stability of *Xenopus laevis* copper,zinc superoxide dismutase. *Arch. Biochem. Biophys*. 377: 284-289.

Bouzyk, E. I., Gradzka, T. Iwanenko, M. Kruszewski, B. Sochanowicz and I. Szumiel. (2000). The responses of L5178Y lymphoma sublines to oxidative stress: antioxidant defense, iron content and nuclear translocation of the p65 subunit of NF-kB. *Acta. Biochem. Pol*. 47: 881-888.

Bravo, J., J.M. Mate, T. Schneider, J. Switala, K. Wilson, P.C. Loewen and I. Fita. (1999). Structure of catalase HPII from *Escherichia coli* at 1.9 A^o resolution. *Proteins* 34: 155-166.

Bricker, B.J., B. A. Tabatabai, B.A. Judge, B. L. Deyoe and Mayfield. (1990). Cloning and expression, and occurrence of the Brucella Cu,Zn superoxide dismuatase, *Infect. Immun*. 58: 2935-2939.

Buettner, G.R. (1998). Antioxidant enzymes and function. Sunrise free radical school for oxygen society. (Electronic publication).

Castellanos-Gonzalez A., L. Jimenez and Landa, A. (2002). Cloning, production and characterization of a recombinant cu/Zn superoxide dismutase from *Taenia solium*. *Int. J. Parasitol.* 32 : 1175-1182.

Ceballos, I., A. Nicole, P. Briand, G. Grimber, A. Delacourte, S. Flament, J.L. Blouin, M. Thevenin, P. Kamoun and P.M. Sinet. (1991). Expression of human, Cu,Zn superoxide dismutase gene in transgenic mice: model for gene dosage effect in Down syndrome. *Free Radic research commun*. 12-13(Pt 2): 581-589.

Chance, B. (1949). The primary and secondary compounds of catalase and methyl or ethyl hydrogen peroxide II kinetics and activity. *J. Biol. Chem*. 179: 1341-1369.

Chen, X., H. Liang, H.V. Remmen, J. Vijg and A. Richardson. (2004). Catalase transgenic mice; characterization and sensitivity to oxidative stress. *Arch. Biochem. Biophys.* 422: 197-210.

Cheng, W., Y.S. Tung, C.H. Liu and J.C. Chen. (2006). Molecular cloning and characterization of cytosolic manganese superoxide dismutase (cytMn-SOD) from the giant freshwater prawn *Macrobacterium rosenbergii. Fish and selfish immunology.* (*in press*).

Church, S. L., J. W. Grant, E. U. Meese and J. M. Trent (1992). Sublocalization of the gene encoding manganese superoxide dismutase (MnSOD/SOD2) to 6q25 by fluorescence *in situ* hybridization and somatic cell hybrid mapping. *Genomics.* 14 : 823-825.

Dadras, S.S., S. Hayashi, J.K. Reddy and A.V. Yeldandi. (1996). Amphibian catalase: cloning, tissue distribution, and peroxisomal localization. *Ann. N.Y. Acad. Sci.* 804: 792-795.

Deisseroth, A. and A. Dounce. (1970). Catalase; physical and chemical properties, mechanism of catalysis, and physiological role. *Physiol. Rev*. 50: 319-375**.**

DiSilvestre, D., S.R. Kleeberger, J. Johns and R.C. Levitt. (1995). Structure and DNA sequence of the mouse Mn SOD gene. *Mamm Genome*. 6:281-284.

Drane P, A. Bravard, V. Bouvard and E. May. (2001). Reciprocal down-regulation of p53 and SOD2 gene expression - implication in p53 mediated apoptosis. *Oncogene.* 20**:**430-439.

Fita, I. and M.G. Rossmann. (1985). The NADPH binding site on beef liver catalase. *Proc. Natl Acad. Sci.* USA 82: 1604-1608.

Fridovich, I. (1986). Superoxide dismutase, *Adv. Enzymol*. 58: 61-97.

Fridovich I. 1995. Superoxide radical and superoxide dismutases. *Annual Review of Biochemistry* 64**,** 97–112.

Forest, K. T., P. R. Langford, J. S. Kroll and E. D. Getzoff. (2000). Cu,Zn superoxide dismutase structure from a microbial pathogen establishes a class with a conserved dimer interface. *J Mol Biol* 296: 145-153.

Fukuhara, R., T. Tezuka and T. Kageyama. (2002). Structure, molecular evolution, and gene expression of primate superoxide dismutases. *Gene.* 296: 99-109.

Geret, F., H. Manduzio, R. Company, F. Leboulenger, M.J. Bebianno and J.M. Danger (2004). Molecular cloning of superoxide dismutase (Cu/Zn-SOD) from aquatic mollusks. *Marine environmental research*. 58: 619-623.

Gerhard, G.S., E.J. Kauffman and M.A. Grundy. (2000). Molecular cloning and sequence analysis of the *Danio reiro* catalase gene. *Comp. Biochem. Physiol. B Biochem. Mol. Biol.* 127: 447-457.

Getzoff, E.D., J.A. Tainer, M.M. Stempien, G.I. Bell and R.A. Hallewell (1989). Evolution of CuZn superoxide dismutase and the Greek key beta-barrel structural motif. *Proteins.* 5:32-336.

Giannopolitis, C.N. and S.K. Rios. (1977). Superoxide dismutase II purification and quantitative relationship and soluble protein in seedlings, *Plant physiol,* 59: 315-318.

Gracia-Gonzalez, A. and J.L. Ochoa (1990). Anti-inflammatory activity of

Debaryomyces hansenii Cu, Zn-SOD. *Arch Med Res*. 30:69-73.

Hallewell R.A., K.C. Imlay, P. Lee, N.M. Fong, E. D. Gallegos, J.A. Getzoff, J.A. Tainer, D.E. Cabelli, P. Tekamp-Olson G. T. Mullenbach and L.S. Cousens. (1991). Thermostabilization of recombinanat human and bovine Cu,Zn superoxide dismutases by replacement of free cysteins. *Biochem. Biophys. Res commun*. 181: 474-480.

Hass, A., K. Brehum, J. Kreft and W. Goeble. (1991). Cloning and characterization and expression of *Escherichia coli* of a gene encoding *Listeria seeligeri* catalase, a bacterial enzyme highly homologus to mammalian cells. *J. Bacteriol.* 173(16): 5159-5167.

Ho, Y.S., A.J. Howard and J.D. Crapo. (1991). Molecular structure of a functional gene for manganese-containing superoxide dismutase. *Am J. Respir . Cell. Mol. Biol*. 4: 278-286.

Jackson , S.M. and Cooper, J.B. (1998) An analysis of structural similarity in the iron and manganese superoxide dismutase based on known structure and sequences. *Biometals* 11: 159-173.

Jeong, J.H., E.S. Kwon and J.H Roe. (2001). Characterization of the Manganese –containing superoxide dismutase and its gene regulation in

stress response of *Schizosacchzromyces pombe*. *Biochemical and Biophysical Research communications,* 283: 908-914.

Kaizer, J., R. Csonka, G. Speier, M. Giorgi and M. Reglier. (2005). Synthesis, structure and catalase-like activity of new dicopper (II) complexes with phenylglyoxylate and benzoate ligands. *J. Mol. Catalysis A: Chemical* 236: 12-17.

Keele Jr., B.B., J.M. McCord and I. Fridovich (1970). Superoxide from *E. coli* B.A. new manganese-containing enzyme. *J. Biol. Chem*. 245: 176-6181.

Ken, C.F., C.C. Lee, K.J. Duan and C.T. Lin (2005). Unusual stability of manganese superoxide dismutase from a new species, *Tatumella ptyseos* ct: its gene structure, expression and enzyme properties. *Protein expression and purification.* 40: 42-50.

Ken, C.F., C.T. Lin, J.F. Shaw and J.L. Wu. (2003). Characterization of Fish Cu/Zn-superoxide dismutase and its protection from oxidative stress. *Mar. Biotechnol.* 5: 167-173.

Kho, D.H., S. B. Yoo, J. S. Kim, E. J. Kim and J. K. Lee (2004). Characterization of Cu- and Zn- containing superoxide dismutase of

Rhodobacter sphaeroides FEMS. *Microbiology letters*. 234: 261-267.

Kim, E.J. H.J. Chung, B. Suh, Y.C. Hah and J.H. Roe. (1998a). Transcriptional and post-transcriptional regulation by nickel of *sod*N gene encoding nickel-containing superoxide dismutase from *Streptomyces coelocolor* Muller. *Mol. Microbiol.* 27 : 187-195.

Kim, E.J. H.J. Chung, B. Suh, Y.C. Hah and J.H. Roe. (1998b) Expression and regulation of the *sod*F gene encoding iron and Zinc-containing superoxide dismutase in *Streptomyces coelocolor* Muller. *J. Bacteriol* 180: 2014-2020.

Kim, Y.H., H.Y. Yoo, G. Jung, J.Y. Kim and H.M. Rho. (1993). Isolation and analysis of the rat genomic sequence encoding Cu/Zn superoxide dismutase. *Gene.* 133 : 267-271.

Kirkman, H.N., S. Galiano and G.F. Gaetani. (1987). The function of catalase-bound NADPH. *J. Biol. Chem*. 262: 660-666.

Kondo, T., H. Terajima, T. Todoroki, T. Hirano, Y. Ito, T. Usia and K. Messmer. (1999). Prevention of hepatic ischemia-reperfusion injury by SOD-DIVEMA conjugate. *J. Surg Res*. 85 (1): 26-36.

Kumar, S., K. Tamura and M. Nei. (2004). Integrated software for molecular evolutionary genetics analysis and sequence alignment, Bioinformatics 5(2): 50-163.

Kwon, S.I. and C.S. An. (2001). Molecular cloning, characterization and expression analysis of a catalase cDNA from hot pepper (*Capsicum annuum* L.). *Plant Sci.* 160: 961-969.

Lebovitz, R.M., H. Zhang, H. Vogel, J. Cartwright Jr., L. Dionne, N. Lu, S, Huang and M. M Matzuk. (1996). Neurodegeneration, myocardial injury, and perinatal death in mitochondrial superoxide dismutase-deficient mice. *Proc. Natl. Acad. Sci.* USA 93: 9782-9787.

Levanon, D., J. Lieman-Hurwitz, N. Dafni, M. Wigderson, L. Sherman, Y. Bernstein, Z. Laver-Rudich, E. Danciger, O. Stein and Y.Groner. (1985). Architechture and anatomy of the chromosomal locus in human chromosome 21 encoding the Cu/Zn superoxide dismutase. *EMBO J* 4: 77-84.

Lin, M.T., T.J. Kuo and C.T. Lin (1998). Molecular cloning of a cDNA encoding copper/zinc-superoxide dismutase from papaya fruit and overexpression in *Escherichia coli*. *J. Agri Food chem*. 46:344-348.

Liu, W., R. H. Zhu, G. P. Li and D. C. Wang (2002). cDNA cloning, high-level expression , purification, and characterization of an avian Cu,Zn superoxide dismutase from Perking duck. *Protein expression and purification* 25: 379-388.

Lowrey, O.H., N.J. Rosebrough, A.L. Farr and R.J. Randoll. (1951). Protein measurement with the folin phenol reagent. *J. Biol. Chem.* 193: 265-275.

McCord, J., and Fridovich, I.: Superoxide Dismutase: The First Twenty Years (1968-1988). (1988). *Free Radic Biol Med* 5: 363-371,

McRee, D.F., S.M. Redford, E.D. Getzoff, J.R. Lepock, R.A. Hallewell and J.A. Tainer. (1990). Changes in crystallographic structure and thermostability of a Cu,Zn superoxide dismutase mutant resulting from the removal of a buried cysteine. *J.Biol.Chem*. 265: 14234-14241.

Melov, S., J.A. Schneider, B.J. Day, D. Hinerfeld, P. Coskun, S.S. Mirra, J.D. Crapo and D.C. Wallace. (1998). A novel neurological phenotype in mice lacking mitochondrial manganase superoxide dismutase. *Nat. Genet*. 18: 159-163.

Meyrick, B. and M.A. Magnuson. (1994). Identification and functional

characterization of the bovine manganous superoxide dismutase promoter. *Am J. Respir. Cell mol Biol.* 10: 113-121.

Moreira, S.F.I., A.M. Bailao, M.S. Barbosa and R.S.A. Jesuino. (2004) Monofunctional catalase P of *Paracoccidiodes brasiliensis*: identification, characterization, molecular cloning and expression analysis. *Yeast.* 21: 173-182.

Motoshima, H., E. Minagawa, F. Tsukasaki and S. Kaminogawa. (1998) Cloning and nucleotide sequencing of genes encoding Mn-superoxide dismutase and class II Fumerase from *Thermus aquaticus* YT-1. *Journal of fermentation and bioengineering.* 86 (1): 21-27.

Muller, H.E. (1985). Detection of hydrogen peroxide produced by microorganism on ABTS-peroxidase medium, Zentralbl. *Bakteriol. Mikrobiyol. Hyg.* 259: 151-158.

Nagai T, I. Inoue, H. Inoue, N. Suzuki (2003). Preparation and antioxidant properties of water extract of propolis. *Food chemistry*. 80: 29-33.

Nakamura, K., M. Watanabe, K. Takanaka, Y. Sasaki and T. Ikeda. (2000) cDNA cloning of mutant catalase in acatalasemic beagle dog; single

nucleotide substitution leading to thermal-instability and enhanced proteolysis of mutant enzyme. *Int. J. Biochem. Cell Biol*. 32: 1183-1193.

Nakano, T., M. Watanabe, M. Sato and M. Takeuchi. (1995). Characterization of catalase from the seaweed *Prophyra yezoensis*. *Plant Sci.* 104: 127-133.

Ni, J., S. Tokuyama, A. Sogabe, Y. Kawamura and Y. Tahara. (2001). Cloning and high expression of catalase gene from *Bacillus sp* TE 124. *J. Biosci. Bioeng.* 91: 422-424.

Oberley, L.W. and G.R. Buettner. (1979) Role of superoxide dismutase in cancer: a review. *Cancer Res.* 39: 1141−1149.

Ogata, M. (1991). Acatalasemia, *Hum. Genet*. 86: 331-340.

Ozturk-Urek R, and L. Tarhan (2001).Purification of superoxide dismutase from chicken liver. *Com. Biochem.Physiol*.Part B 128: 205-212.

Pani, G., B. Bedogni, R. Anzevino, R. Colavitti, B. Palazzotti, S. Borrello and T. Galeotti. (2000). Resistance to Oxidative Injury in p53-deficient Cells. *Cancer Res.* 60: 4654-4660.

Reveillaud, I., A. Niedzwiecki, K.G. Bensch and J.E. Fleming.(1991) Expression of bovine superoxide dismutase in *Drosophila melanogaster* augments resistance of oxidative stress. *Mol Cell. Biol*. 11: 632-640.

Rigo, A., P. Viglino, G. Rotilio and R. Tomat. (1975). Effect of ionic strength on the activity of bovine superoxide dismutase. *FEBS Lett.* 50: 86-88.

Shull, S., N.H. Heintz, M. Periasamy, M. Manohar, Y.M. Janssen, J.P. Marsh and B.T. Mossman. (1991). Differential regulation of antioxidant enzymes in responses to oxidants. *J. Biol. Chem*. 266: 24398-24403.

Smith, M.W. and Doolittle, E.F. (1992). A comparison of evolutionary rates of the two major kinds of superoxide dismutase. *Journal of Molecular evolution.* (1992). 34: 175-84.

Stallings, W.C., K.A. Pattridge, R.K. Strong and M.L. Ludwig. (1985). The structure manganese superoxide dismutase from *Thermus therm* HB8 at 2.4-A0 resolution. *J.Biol. Chem*. 260:16424-16432.

St Clair, D.K., T. D. Oberley and Y.S. Ho. (1991). Overproduction of human Mn- superoxide dismutase modulates paraquat-mediated toxicity in mammalian cells. *FEBS Lett*. 293:199-203

Thuy, L.H.A., K. Phucharoen, A. Ideno and T. Maruyama. (2004). Alkali and Halo–tolerent catalase from *Halomonas sp* SK1: overexpression in *Escherichia coli*, purification, characterization, and genetic modification. *Biosci. Biotechnol. Biochem.* 68 (4): 814-819.

Wan, X. S., M.N. Devalaraja and D.K. St.Clair. (1994). Molecular structure and organization of the human manganese superoxide dismutase gene. *DNA cell Biol.* 13: 1127-1136.

Wang, Z., Z. He, S. Li and Q. Yuan. Purification and partial characterization of Cu,Zn containing superoxide dismutase from entomogenous fungal species *cordyceps militaris*. *Enzyme and Microbial technology*. 36: 862-869.

Wilde, L.G. and M. Yu. (1998). Effect of fluoride on superoxide dismutase (SOD) activity in germinating mung bean seedlings, *Fluoride* 31: 81-88.

Wispé, J. R., B. B. Warner, J. C. Clark, C. R. Dey, J. Neuman, S. W. Glasser, J. D. Crapo, , L-Y. Chang and, J. A. Whitsett. (1992). Human Mn-superoxide dismutase in pulmonary epithelial cells of trangenic mice confers protection from oxygen injury. *J. Biol. Chem*. 267**,** 23937–23941.

Wright, A. C., H. Ahmed, J.D. Gauthier, A.M. Silva and G.R. Vasta. (2002) cDNA cloning and characterization of two iron superoxide dismutase from the oyster parasite *Perkinsus marinus*. *Molecular & Biochemical Parasitology.*123: 73-77.

Xiang, H., W.Z. Wei, H.R. Tan and S.X. Guo. (2000). Cloning and expression of human Cu,Zn superoxide dismutase gene in *Lactobacillus lactis Chin. J. Biotechnol*. 16: 6-9.

Yamamoto, K., Y. Banno, H. Fujii, F. Miake, N. Kashige and Y. Aso. (2005). Catalase from the silkworm, *Bombyx mori*: Gene sequence, distribution, and overexpression. *Insect Biochem. Mol. Biol.* 35: 277-283.

Zamocky, M. and F. Koller. (1999) Understanding the structure and function of catalase: clues from molecular evolution and in vitro mutagenesis. *Prog. Biophys. Mol. Biol.* 72: 19-66.

Zelko, I.N., T.J. Mariani and R.J. Folz. (2002). Superoxide dismutase multigene family: A comparison of the Cu-Zn SOD (SOD1), Mn-SOD (SOD2) and EC-SOD (SOD3) gene structures, evolution and expression. *Free radical biology and medicine*. 33: 337-349.

ACKNOWLEDGEMENT

I am sincerely grateful to Prof. Jehee Lee for his guidance, encouragement and kindness extended to me throughout my study period in South Korea. I owe Prof Sung-Chul Chung for being my supervisor. I wish to express my gratitude to Prof. Yu-Jin Jeon for all the helpful discussions and advices. Prof. Choon- Bok Song, Prof. In-Kyu Yeo, Prof. Moon-Soo Heo, Prof. Kwang-Sik Choi, Prof Young-Don Lee, Prof. Geun-Tae Park and their laboratory staff are gratefully acknowledged for allowing to use their laboratory facilities. A special “thank you” goes to Dr. Nalin Siriwadhana for introducing me to South Korea. Chul-hong Oh, Hyun-Sil Kang and Chamilani Nikapitiya are much appreciated for the endless support extended to me in various ways. I thank all my present and ex-lab members and all Sri Lankan students in Cheju National University for being very helpful and encouraging. Brain Korea 21 program is gratefully acknowledged for the financial assistance given and the support given by the staff of the Graduate School of Cheju National University is also acknowledged. I am also grateful to Dr. K.H. Sarananda of Food Research Unit, Gannoruwa, Sri Lanka for encouraging me for research and higher studies. Last, but not least, a debt of gratitude is also owed to my loving parents, parents-in-law and my dear husband, Shamilka Ekanayake for being the source of strength and inspiration for all my work.